Depositional Environment and Hydrocarbon Potential of Coal and Oil Shale in the Lower Miocene Aleksinac Basin (Serbia)

Klaus Oberauer, BSc

Univ.-Prof. Mag.rer.nat. Dr.mont. Reinhard F. Sachsenhofer

Chair of Petroleum Geology

University of Leoben

A thesis submitted for the degree of

Master of Science

March 2017

Affidavit:

I declare in in lieu of oath, that I wrote this thesis and performed the associated research myself, using only literature cited in this volume.

Eidesstattliche Erklärung:

Hiermit erkläre ich an Eides statt, dass ich die vorliegende Masterarbeit selbstständig verfasst, keine anderen als die angeführten Quellen verwendet und die wörtlich oder inhaltlich entnommenen Stellen als solche kenntlich gemacht habe.

Leoben, March 2017

Klaus Oberauer

Acknowledgments

First, I would like to thank my supervisor Reinhard Sachsenhofer for his guidance throughout the process of writing this thesis.

Secondly, I would like to extend my gratitude to Aleksandar Kostic and the University of Belgrade for providing me with the samples and data which made this project possible.

Special thanks go to Doris Groß for introducing me into the secrets of source rock analysis and organic petrography. I also want of thank Achim Bechtel and Reinhard Gratzer for helping me with the laboratory work, sharing with me their knowledge on biomarkers and giving me advice in evaluation and interpretation of geochemical data. I also want to mention the funny times and nice talks with Sabine Feuchter during sample preparation.

I would like to express my gratitude to Ursula Schmid for all her support in administrative affairs.

I want to thank my colleagues at the chair of Petroleum Geology, especially Magdalena Pupp, Bernhard Rupprecht and Johannes Rauball for all their help, support and motivating words during my work on the thesis.

I really appreciate the time I could spend with my friends and all the crazy things we did together. All of you made my stay in Leoben to a really special one.

Last but not least, very, very special thanks goes to my parents, Wolfgang and Christa Oberauer, supporting me during my entire studies and encouraging me also in times of less success.

Abstract

Numerous sedimentary basins with oil shale deposits occur in Serbia. Their formation and development was controlled by tectonic cycles, which also influenced the formation and development of the southern part of the Pannonian Basin. The most important oil shale deposit is located in the Aleksinac Basin and is assigned to the Lower Miocene.

A lower and an upper oil shale horizon occur in the Aleksinac Basin, which are separated by the several meter thick "Aleksinac" coal seam. The lower oil shale horizon has a thickness of 30 m and includes interlayered sandy rocks and thin coal layers. The upper oil shale layer overlies the Aleksinac coal seam and is about 60 m thick. Intensive faulting by the end of the Early Miocene divided the deposit into tectonic blocks with various dip angles.

In this study the depositional environment of the Aleksinac coal seam and of the upper oil shale layer was investigated. In addition, the hydrocarbon potential of the sedimentary succession in the Aleksinac Basin was quantified. The study outcomes are based on bulk geochemical, organic petrographical, organic geochemical as well as carbon-isotope data of samples taken from well BD-4, which was drilled near the village of Subotinac. Different biological markers, including *n*-alkanes, isoprenoids, steroids, hopanoids, di- and triterpenoids, were determined.

Maturity parameters, such as vitrinite reflectance and temperature of maximal hydrocarbon generation (T_{max}), indicate that the organic material is thermally immature. The Aleksinac coal seam in the well BD-4 is around 4 m thick and was deposited subaqueously in a low-lying mire. The plant input is dominated by angiosperms. The upper part displays an unusual high HI (> 500 mgHC/gTOC) for a coal seam. A relative rise in water level led to the drowning of the swamp and to the deposition of the 60-m-thick upper oil shale in a lacustrine environment. The organic material of the oil shale is dominated by algae and bacterial biomass and, therefore, is classified as type I kerogen. Biomarker data suggest a stratified water column which likely was formed due to differences in salinity. The stratified water column led to a strictly anoxic environment in a mesosalinar lake which enabled the accumulation of uncommon high amounts of organic material (average TOC: 18.0 wt.%) and excellent preservation (average HI: 743 mgHC/gTOC).

TOC and Rock-Eval data show, that the lower and upper oil shale layers are "excellent" source rocks and that they can generate 7.8 tons of hydrocarbon per m^2 (t HC/m^2, lower oil shale) and 14.2 t HC/m^2 (upper oil shale), respectively. The oil yield is about 15 wt.% in the lower oil shale and about 12 wt.% in the upper oil shale.

Kurzfassung

In Serbien gibt es eine Vielzahl von Sedimentbecken mit Ölschieferlagerstätten, die bis dato in unterschiedlicher Genauigkeit exploriert wurden. Sie wurden von einer Reihe tektonischer Vorgänge geprägt, welche auch die Bildung und Entwicklung des Pannonischen Beckens beeinflussten. Die wichtigste Ölschieferlagerstäte befindet sich im Aleksinac Becken und wird in der Literatur dem Untermiozän zugeordnet.

Im Aleksinac Becken treten ein oberer und ein unterer Ölschieferhorizont auf, welche durch ein mehrere Meter mächtiges Kohleflöz voneinander getrennt werden. Der untere Horizont hat eine Mächtigkeit von 30 m und alterniert mit siliziklastischen Sedimenten und dünnen Kohlelagen. Der obere Ölschieferhorizont liegt mit einer Mächtigkeit von 60 m direkt dem Aleksinac Kohleflöz auf. Intensive Tektonik am Ende des Untermiozäns hat die Lagerstätte in tektonische Blöcke mit unterschiedlichen Einfallswinkeln geteilt.

In dieser Studie wurde der Ablagerungsraum des Aleksinac Kohleflözes und des oberen Ölschieferhorizontes untersucht und das Kohlenwasserstoffpotential der gesamten Schichtfolge im Aleksinac Becken quantifiziert. Die Ergebnisse basieren auf Elementaranalysen, Rock-Eval Pyrolyse, organischer Petrologie, organischer Geochemie sowie Kohlenstoff-Isotopie. Zudem wurden biologische Marker wie *n*-Alkane, azyklische Isoprenoide, Sterane, Hopane, Diterpane, Triterpane und eine Reihe anderer Biomarker bestimmt. Analysiert wurden Proben unterschiedlicher Lithologien aus der Bohrung BD-4 in der Nähe des Ortes Subotinac.

Maturitätsparameter wie Vitrinitreflexion und Temperatur der maximalen Kohlenwasserstoffgeneration (T_{max}) zeigen, dass das organische Material thermisch unreif ist. Das Aleksinac Kohleflöz in der Bohrung BD-4 ist ca. 4 m mächtig und wurde subaquatisch abgelagert. Der Pflanzeneintrag wurde durch Angiospermen dominiert. Der obere Teil weist einen für Kohleflöze ungewöhnlich hohen HI (>500 mgKW/gTOC) auf. Ein Anstieg des Seespiegels führte zum Ertrinken des Moores und zur Ablagerung des ca. 60 m mächtigen oberen Ölschiefers. Das organische Material des Ölschiefers wird von Algen und Bakterien dominiert und somit als Kerogentyp I klassifiziert. Biomarkerdaten weisen auf einen geschichteten Wasserkörper hin. Die Wassersäulenschichtung resultierte vermutlich von unterschiedlicher Salinität und führte zu strikt anoxischen Verhältnissen in einem mesosalinaren See, die die Akkumulation von ungewöhnlich hohen Mengen an organischem Material (durchschnittlicher TOC: 18.0 Gew.%) mit ausgezeichneter Erhaltung (durchschnittlicher HI: 743 mgKW/gTOC) ermöglichten.

TOC und Rock-Eval Werte zeigen, dass der untere Ölschieferhorizont und der obere Ölschieferhorizont ein „exzellentes" Muttergesteinspotential aufweisen und 7.8 Tonnen Kohlenwasserstoffe je m² (t KW/m²; unterer Ölschiefer), bzw. 14.2 t KW/m^2 (oberer Ölschiefer) generieren können. Der Schieferölausbeute wird mit ca. 15 Gew.% (unterer Ölschiefer), bzw. 12 Gew.% (oberer Ölschiefer) abgeschätzt.

Contents

1. Introduction

Organic matter rich rocks including oil shale and coal provide great archives for paleoenvironmental conditions. Such rocks often form an essential part of the fill of lacustrine, fault-controlled sedimentary basins and may represent excellent petroleum source rocks (Caroll and Bohacas, 1999; Sachsenhofer et al., 2003). The sedimentary successions of tectonically controlled basins are typically characterized from bottom to top by fluvial sediments, a single thick coal seam and lacustrine rocks (Lambiase, 1990; Sachsenhofer, 2000).

In Serbia, many lacustrine basins were formed during different tectonic phases between Oligocene to Pliocene times. The basins are associated with local crustal extension or transtension causing high subsidence rates (Marovic et al., 1999). A significant number of these basins hosts oil shale deposits (Figure 1.1).

This master´s thesis focuses on the Aleksinac Basin, located about 200 km southeast of Belgrade in the Serbo-Macedonian Metallogenic Province (Figure 1.1). The Aleksinac Basin is filled by Lower and Upper Miocene sediments. The Lower Miocene sediments (Aleksinac series), up to 800 m thick, include from base to top fluvial sediments, marginal lacustrine sediments with oil shale and several coal seams, and an intrabasinal facies (Bituminous Marl). Oil shale layers occur within the marginal lacustrine facies and are separated into a lower and an upper productive horizon by the main Aleksinac coal seam (Petkovic & Novkovic, 1975; Jelenkovic et al., 2008). The Upper Miocene sediments (Red Clastic series) follow above a major unconformity.

Main study aims are to reveal vertical variations in amount and type of organic matter, to determine the source rock potential and to reconstruct the depositional environment of oil shale and the main Aleksinac coal seam. The study is based on samples taken from the exploration well BD-4/2011, drilled 9 km north of the town of Aleksinac. Because it cannot be excluded that the lower part of the Aleksinac series beneath the Aleksinac coal seam is disturbed by faults in the studied borehole, the present investigation focuses on the upper oil shale layer.

To reach the goal, bulk geochemical parameters (total organic carbon [TOC], total inorganic carbon [TIC], sulphur [S]; Rock-Eval) as well as organic geochemical (biomarkers; carbon isotopy) and organic petrographical (macerals, vitrinite reflection) parameters were determined.

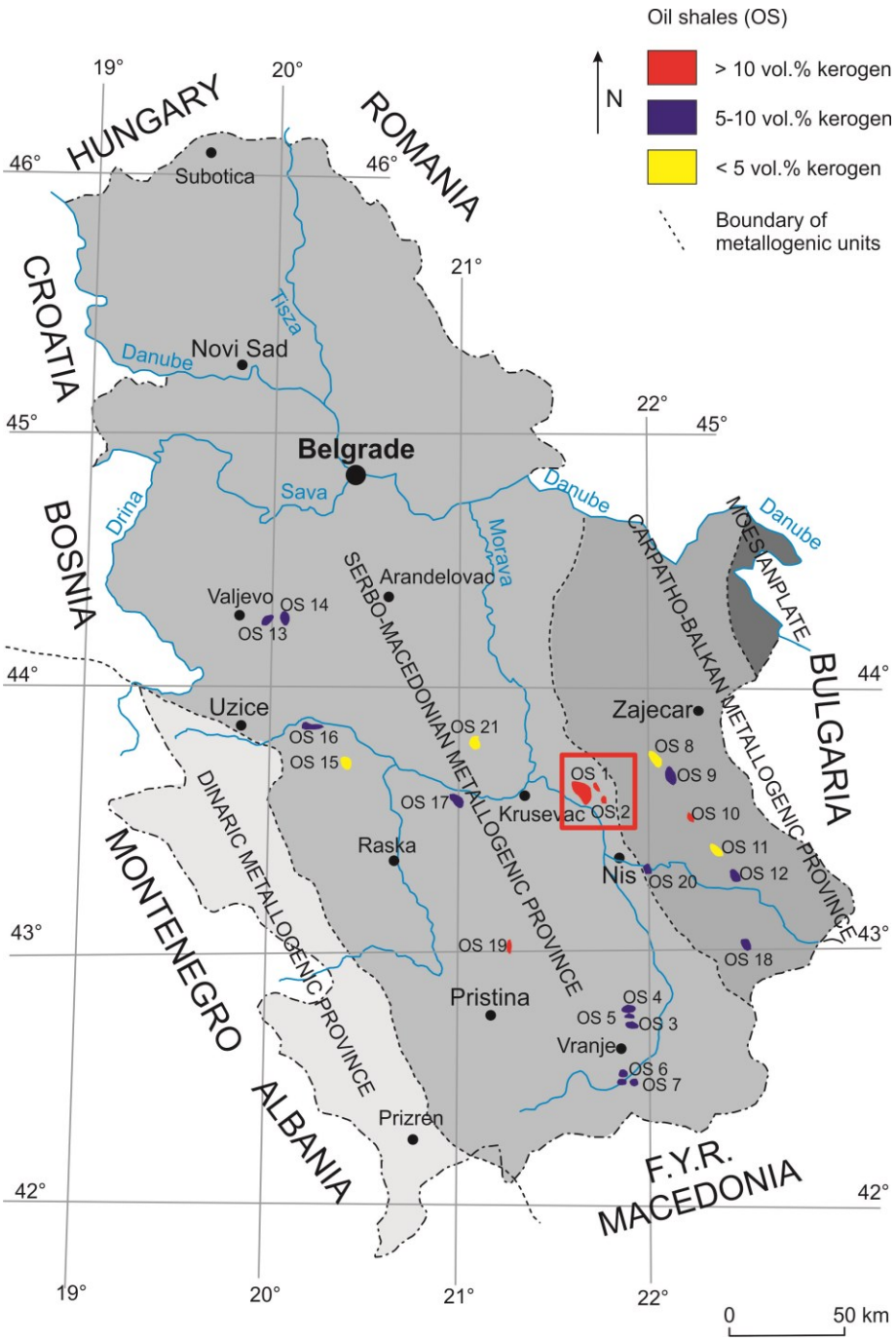

Figure 1.1: Oil shale deposits in Serbia (modified after Ercegovac et al., 2009). OS 1. Aleksinac deposit; OS 2. Bocan-Prugovac; OS 3. Goc-Devotin deposit; OS 4. Vlase-G.Selo; OS 5. Stance; OS 6. Bustranje; OS 7. Klenike; OS 8. Vlasko polje-Rujiste; OS 9. Vina-Zubetinac; OS 10. Podvis-Gornji Karaula; OS 11. Manojlica-Okoliste; OS 12. Miranovas-Orlja; OS 13. Suseoke-Klasnic; OS 14. Radobicka Strana-Svetlak; OS 15. Pekcanica-Lazac; OS 16. Parmenac-Lazac; OS 17 Odzaci; OS 18. Raljin; OS 19. Raca; OS 20. Paljina; OS 21. Komarane-Kaludra. Basic data of these deposits are shown in Table 1.1

1.1 Oil shales

According to Savage (1967) the term "oil shale" is a misnomer because it is neither truly shale nor does it generally have any oil in it. A more suitable name would be organic marlstone and he noted that "oil shale" is only a promotion term: "The magic word 'oil' would raise large sums of promotion money while organic marlstone wouldn't raise a dime."

Per definition in literature oil shale refers to a fine-grained sedimentary rock with high contents in thermally immature organic matter (called kerogen) that is released as petroleum-like liquids when the rock is heated in the chemical process of pyrolysis (Dyni, 2006). Oil shale can be a potential source rock that would have generated petroleum and natural gas, if it had been subjected to geological burial at required temperature and pressure for sufficient time (Allix et al., 2011).

Otherwise oil shale deposits which have not been exposed to excessive heating are geothermally immature, but close enough to the surface to be mined by open-pit, underground mining or in-situ methods (Dyni, 2005). Extracting the oil from the shale can be much more complicated and expensive than conventional oil recovery. Various steps, including mining and crushing have to be carried out before the oil shale can be transported to surface facilities. There it is heated up to a high temperature to convert kerogen to oil and gas and to separate the hydrocarbon fraction from the mineral fraction. Alternative methods have been tested to heat the rock in situ and extract the shale oil in a more conventional way through boreholes (Allix et al., 2011). Shell Oil for example has developed an in situ conversion process (ICP), where underground oil shale is heated up over a period of approximately four years until it reaches 340-370°C using electric heaters placed in deep vertical wells drilled through a section of oil shale. Kerogen is slowly converted into shale oil and gases, which are transported to the surface through recovery wells (Bartis et al., 2005). Also ExxonMobil is pursuing research targeting at the development of a process for in situ oil shale conversion. More about their Electrofrac process creating a resistive heating element can be obtained from Symington et al. (2010). It is important to note that all of those current projects to produce shale oil by in situ heating methods are in test and pilot stages and operators are still working to optimize their heating technologies. Due to environmental impacts (e.g. groundwater pollution, mechanical stability) and currently unfavourable economic conditions most of those projects are difficult to realize (Allix et al., 2011).

Oil shales are formed in a variety of depositional environments, including near-shore marine basins and subtidal shelves, fresh-water to saline lakes, and swamps which are commonly associated with deposits of coal. Predominantly the organic matter in oil shales is derived from various types of marine and lacustrine algae. Minor amounts are varied mixtures of spores, pollen, plant cuticle and corky fragments of herbaceous and woody plants, dependent on the depositional environment and geographic position (Dyni, 2005).

Oil shales can occur in thin layers or in giant accumulations hundreds of meters thick and are spread in more than 30 countries worldwide. The most important deposits are located in the United States, Russia, Democratic Republic of Congo, Brazil, Italy, Morocco, Jordan and China. It is expected that these deposits would yield at least 40 litres of shale oil per metric ton of oil shale (Dyni, 2005). Resources of the world's shale oil are about 3.2 trillion barrel (bbl) whereby 60% of this amount is located in the US (Knaus et al., 2010).

1.2 Previous research on oil shale basins in Serbia

According to Cokorilo et al (2009), Serbia has relatively few shale oil resources (estimated 2.08 billion bbl; calculated with an oil density of 0.8617 t/m^3) compared to the United States. The assessment of the amount of shale oil is based on oil yield analyses according to the Fischer method. Geological exploration resulted in the detection of 21 oil shale deposits with varying quality and oil yield. Most of them are in Paleogene to Miocene basins. However, these deposits are explored on various levels. Because only two of them are explored in detail (Aleksinac deposit and Goc-Devotian deposit), most of the oil shale potential in Serbia should be considered in terms of resources instead of reserves. The 10 most important oil shale basins are Aleksinac, Vranje, Senonian Trench, Valjevo-Mionica, Western Morava, Krusevac, Babusinaca, Kosanica, Nis and Levac (Cokorilo et al., 2009). The locations of the different deposits are shown in Figure 1.1, basic parameters are listed in Table 1.1.

The economically most important deposit is located about 200 km southeast of Belgrade in the Aleksinac Basin (red rectangle in Figure 1.1) and extends over an area of more than 20 km^2. The Aleksinac oil shale deposit is known for more than 100 years because of extensive coal mining, which started in 1883. The Aleksinac coal mine was closed in 1990. Interest in the Aleksinac oil shale increased during the 1980s. Nevertheless, the deposit is not in exploitation yet, but test production has shown that the expected yield might be about 80 kg of oil and 400 m^3 of gas per ton of shale (Ercegovac et al., 2009). According to Cokorilo et al. (2009), the Aleksinac deposit contains reserves of 1.46 billion bbl shale oil and is therefore the most important one in Serbia. Based on preliminary data collected by the University of Belgrade (Faculty of Mining and Geology) and the Viru Keemia Grupp AS (VKG; Estonia), Cokorilo et al. (2009) concluded that the oil shale in the Aleksinac Basin can be mined by surface and underground mining methods and that it can be thermally processed using existing commercial technologies. Organic geochemical investigations on Aleksinac oil shale have been performed by Kasanin-Grubin et al. (1997), Vass et al. (2006) and Ercegovac et al. (2009). Jelenkovic et al. (2008) emphasize that the Aleksinac coal is sub-bituminous in rank and rich in liptinite macerals. The Bovan-Prugovac deposit is the second deposit which is located in the Aleksinac Basin. The oil shale has an thickness between 10 and 33 m with an oil yield of 6 wt.%. Estimated shale oil reserves are 92 million bbl.

The Senonian Tectonic Trench has significant occurrences of oil shale and is located in the Carpatho-Balkan Metallogenic Province (Figure 1.1). This basin includes the Vina-Zubetin deposit as the second largest one in Serbia with a predominating lamosite type of oil shale. The thickness of the oil shale is between 20 and 80 m. It contains 5.4 vol.% organic matter and has an oil yield of 2.6 wt.%. Shale oil reserves run up to 161 million bbl. The oil shale of the Podvis-Gornji Karaula deposit is characterised by an average oil yield of 7.5 wt.%, which makes the deposit very interesting. Unfortunately, oil layers are thin, mainly below 1 m (Cokorilo et al., 2009).

Another important oil shale basin is the Vranje basin, located in the south of Serbia (Figure 1.1). It consists of several oil shale deposits, where the best explored one is the Goc-Devotian. This deposit is, like the Aleksinac deposit, divided into a lower and upper oil shale package. The lower package, 2 to 6 m thick, has an average content of organic substance of 5.9 vol.% and an average oil yield of 2.1 wt.%. The thickness of the upper oil shale package ranges from 10 to 23 m, with average content of organic substance of 8.8 vol.% and an average oil yield of 4.5 wt.%. Shale oil reserves in the upper and lower package are 9.5 million bbl.

Table 1.1: Basic data of oil shale deposits in Serbia (modified from Cokorilo et al., 2009). 1 bbl ≈ 0.137 metric tons of oil (ρ_{oil} =0.8617 t/m^3)

Basin	Deposit	Thickness (m)	Average thickness (m)	Average content		Reserves/Resource		
				Kerogen vol.%	Oil yield (Fischer assay) wt.%	Shale (10^6 t)	Oil (10^6 t)	Oil (10^6 bbl)
Aleksinac	Aleksinac	54–92	75.5	20.0	10.0	2000	200	1460
		7–29	20.2	25.0	12.5	–	–	–
	Bovan-Prugovac	10–33	20.0	12.2	6.0	210	12.6	92
Vranje	Goč-Devotin	10–23	15.0	8.8	4.5	22	1.0	7.3
		2–6	3.9	5.9	2.1	13.8	0.3	2.2
	Vlase-Golemo Selo	6–13	9.7	5.5	3.4	38.5	1.3	9.5
		3–7	4.4	2.5	1.4	–	–	–
	Stance	–	4.0	5.6	2.6	45	1.2	8.8
		–	6.0	6.2	2.6	–	–	–
	Buštranje	4–13	9.0	8.2	3.4	46	1.6	11.7
		5–9.5	7.0	5.0	1.4	36	0.5	3.7
		4.2–9.0	6.0	5.2	1.4	30	0.4	2.9
	Klenike-Jastina Bara	1.3–13	7.5	5.6	3.4	42	1.4	10.2
		1.5–10	6.0	6.7	3.2	30	1.0	7.3
		9–11	10.0	5.2	1.3	–	–	–
	Baraljevac	4–6	5.6	7.3	2.8	8	0.2	1.5
	Drežnica	8–10.7	9.0	8.5	5.1	35	1.8	13.1
		–	7.5	8.4	4.9	30	1.5	11.0
Senonian Trench	Veliko Polje-Rujiš	20–150	72.0	–	0.5	–	–	–
	Vina-Zubetin	20–80	31.0	5.4	2.6	850	22.1	161
	Podvis-Gornji Kar.	2–5	4.0	–	7.5	10	0.1	0.7
	Miran.-Orlja	5–33	12.0	4.5	2.2	70	1.5	11.0
	Man.-Okoliš	10–35	25.0	5.1	2.4	100	2.4	17.5
Valjevo-Mionica	Šuše-Klasnić	5–15	9.0	7.2	3.2	30	1.0	7.3
	Rad. Str. Svet.	4–15	9.0	8.4	3.9	80	3.1	22.6
Western Morava	Pekcanica-Lazac	–	4.4	5.0	1.3	38	0.3	2.2
		–	1.7	3.0	0.9	–	–	–
	Paramenac-Riđage	–	2.3	6.0	1.3	18	0.2	1.5
		–	2.7	3.3	0.8	–	–	–
Kruševac	Odžaci	3–11	7.0	6.8	1.7	20	0.3	2.2
Babušnica	Raljin	24–40	30.0	7.4	3.7	300	9.6	70
		9–15	12.0	5.2	2.6	–	–	–
Kosanica	Rača	4–6	4.4	11.5	5.2	20	1.0	7.3
		1–2	1.4	3.6	1.6	–	–	–
Niš	Paljina	–	15.0	–	3.2	500	16.5	120
		–	6.0	–	3.3	–	–	–
Levač	Komarane-Kaludra	–	7.0	3.4	0.6	190	1.9	13.8
		–	2.0	3.0	1.4	–	–	–
						4812.3	**284.8**	**2078.3**

2. Geological Setting of the Aleksinac Basin

Different tectonic events resulted in formation of lacustrine basins in the territory of present-day Serbia, especially between Oligocene and Pliocene time. Those tectonic movements were genetically related to the formation and evolution of the Pannonian Basin (Obradovic et al., 2000). The tectonic activity led to the formation of numerous lacustrine basins with diverse sediments. The lacustrine sediments are alternating with alluvial and swamp deposits which represent different facies zones. It is characteristic that the basins have mostly NNW-SSE direction (Obradovic et al., 1997). The Aleksinac Basin is located south of the Pannonian Basin (Peri Pannonian Realm), where three geotectonic units were formed due to compressional forces occurring during convergence of several oceanic and continental units between the African and European plates: Dinarides, Serbian Macedonian Massif and Carpatho-Balkanides (Figure 2.1 inset (B)).

At the Cretaceous/Palaeogene boundary all of the subduction-collisional processes in these terrains were largely completed. Individual basins within the southern rim of the Pannonian Basin were connected to local crustal extensions, i.e. tensional processes and normal faulting as well as to two stage subsidence. In the first Ottnangian-Karpatian-Badenian stage, subsidence was mostly the result of crustal and lithospheric extension (syn-rift phase). It was characterized by fast subsidence and bounded to faulted areas. The syn-rift phase was followed by a Late Miocene to Pliocene post-rift phase. This subsidence was slower and caused by cooling and contractions of the lithosphere (Marovic et al., 2002).

Under such circumstances also the Aleksinac Basin was formed. This basin is located 200 km southeast of Belgrade and covers the area between the South Morava river and its right affluence Moravica. The oil shale deposit in the basin was discovered between the cities of Aleksinac and Subotinac in a 1.5 to 2.5 km wide and 8 km long belt. It covers an area of more than 20 km^2 and belongs to the Serbo-Macedonian Metallogenic Province (Ercegovac et al., 2009).

The three fields of the Aleksinac deposit "Dubrava", "Morava" and "Logoriste" are displayed in Figure 2.2 (Gajica et al., 2016). The analysed samples are from the deviated borehole BD-4/2011 in the Dubrava field (1.5 km northwest of Subotinac) marked with a blue arrow in Figure 2.3.

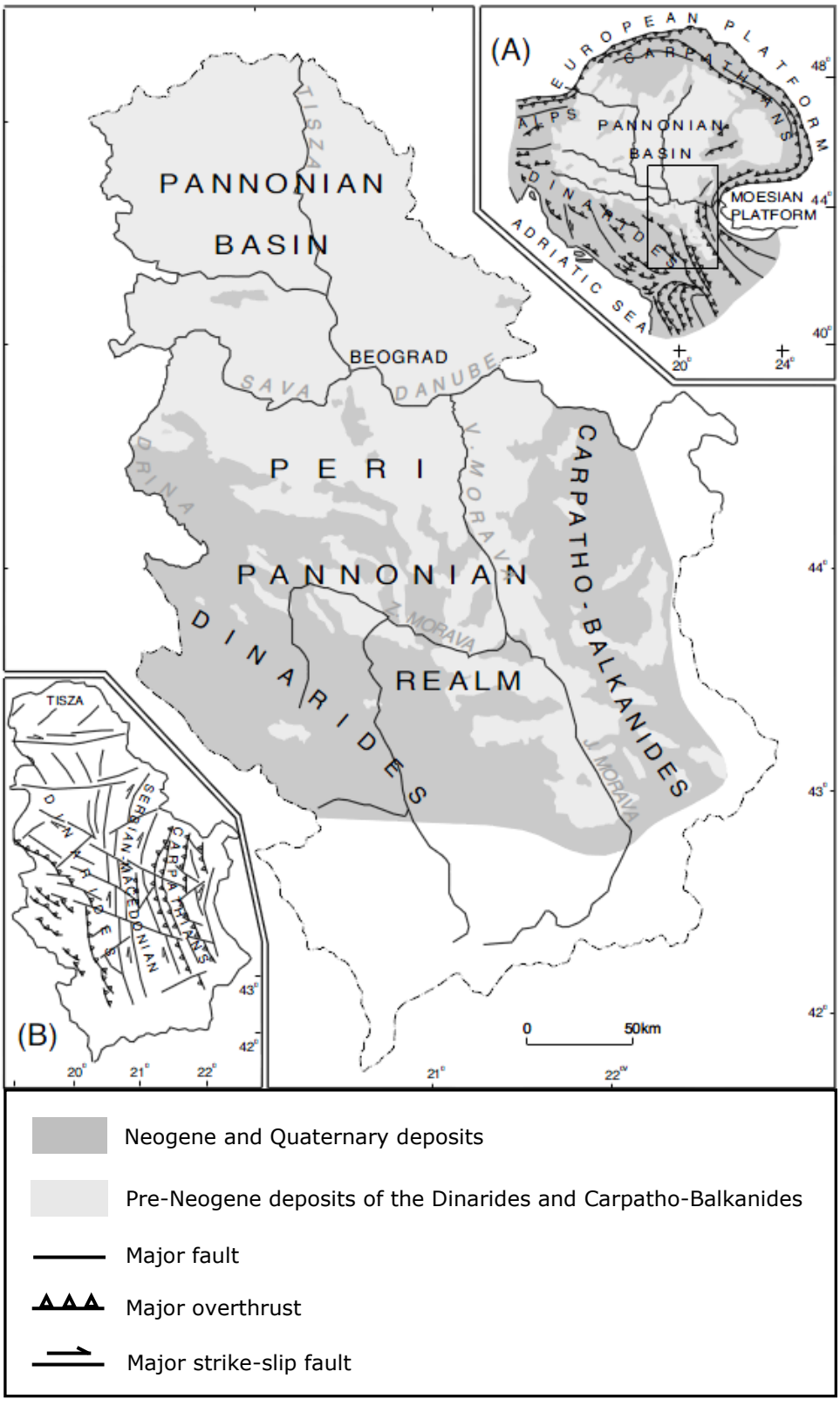

Figure 2.1: Simplified geological map of the Serbian part of the Pannonian Basin. Inset: (A) position of the study area within the European Alpides and (B) major tectonic units of the Serbian part of the Pannonian Basin (Marovic et al., 2002)

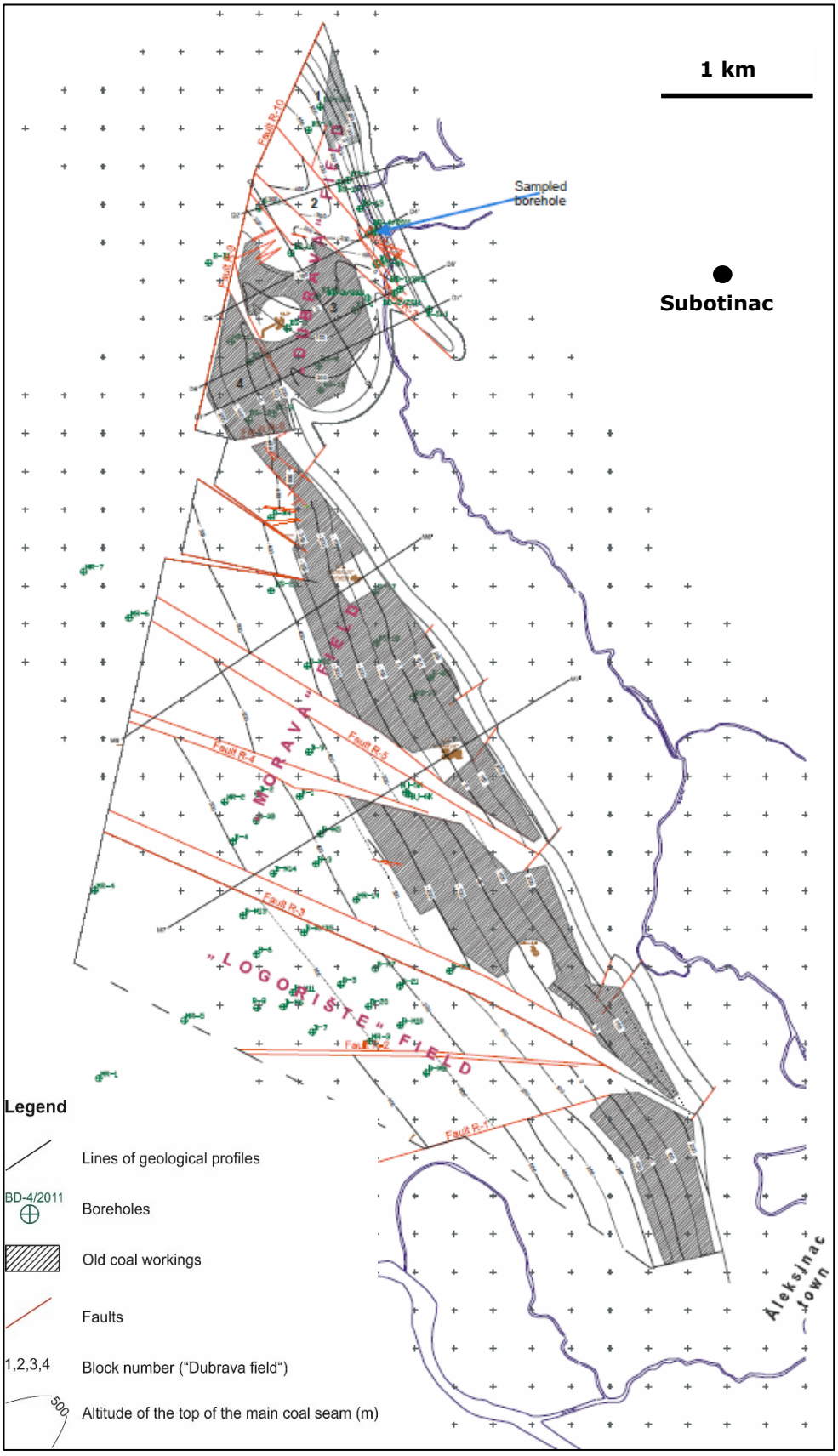

Figure 2.2: Three main fields of the Aleksinac deposit according to Kostic (2016)

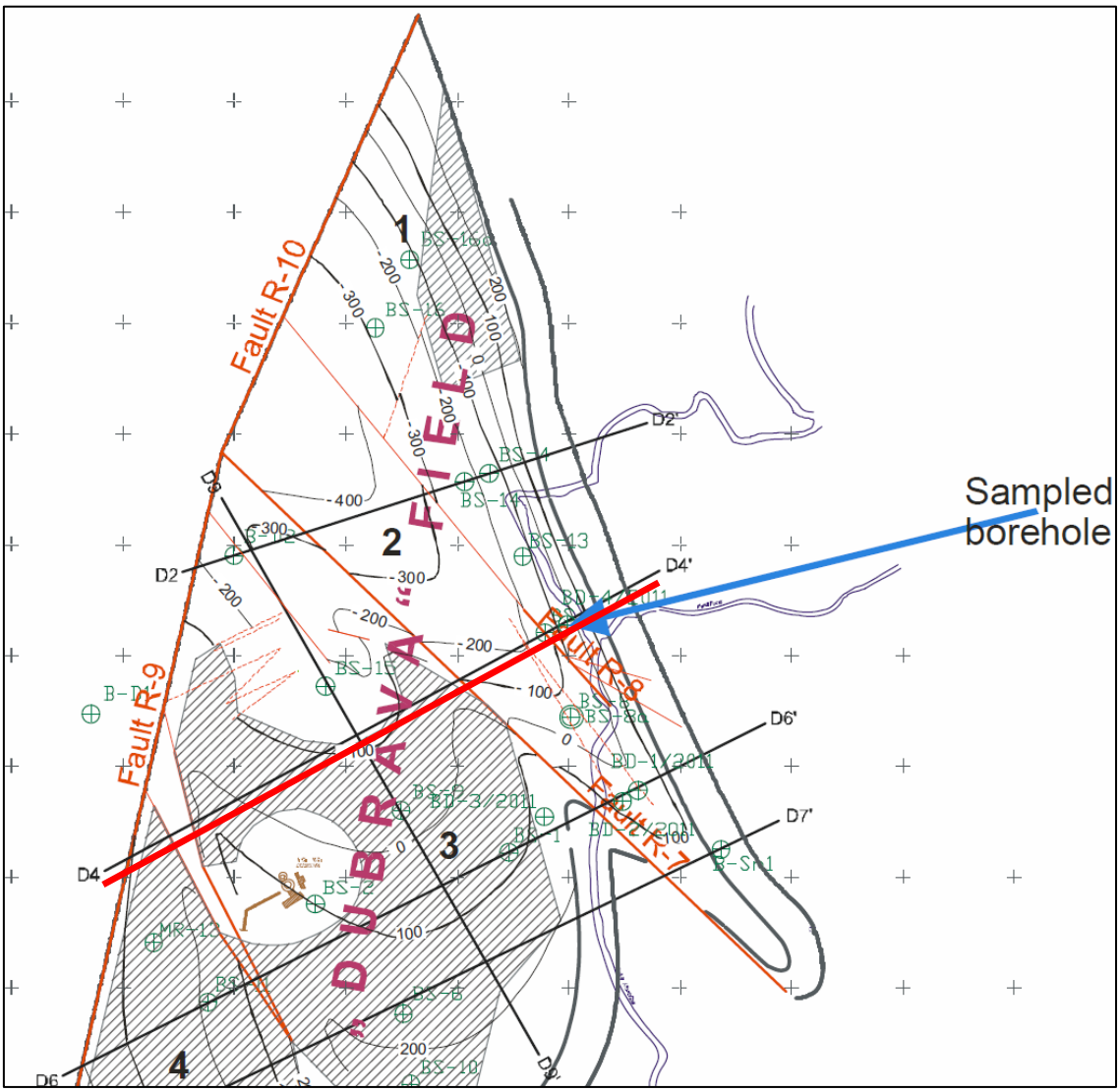

Figure 2.3: Location of the analysed samples in the Dubrava Field, 1.5 km northwest of Subotinac town according to Kostic (2016)

2.1 Stratigraphy

The age of the fill of the Aleksinac Basin is poorly constrained. However, it is generally accepted that the basin is filled by a Lower Miocene sedimentary complex (Aleksinac series) which is discordantly covered by Upper Miocene sediments (Red Clastic series; e.g. Kasanin-Grubin et al., 1997 and references therein). While the alluvial to lacustrine Aleksinac series is often fine-grained and up to 800 m thick, the Red Clastic series consists of coarse-grained clastic rocks including conglomerate, sandstone and clayey sandstone and is up to 700 m thick (Ercegovac et al., 2009).

According to previous sedimentological analysis four different facies were distinguished in the Lower Miocene Aleksinac series (Figure 2.4). The basal series is formed by an alluvial facies and is represented by reddish clastic sediments including coarse grained, weakly cemented conglomerate, conglomeratic sandstone and claystone. It rests directly on crystalline schists of Precambrian to Cambrian age. The lower part of the marginal-lacustrine facies is represented by well-bedded fine-grained sandstones and siltstones. The sandstones are classified as sub-arkoses and often cemented by calcite. These rocks also contain coalified plant particles and lithoclasts of volcanic rocks. The main part of the marginal-lacustrine facies contains two layers of oil shale with the main Aleksinac coal seam between them. The coal seam, 2 to 6 m thick, represents the swamp facies. While the lower oil shale layer is alternating with siliciclastic rocks like clayey and mica sandstone and some thin coal lenses with thicknesses from 0.2 to 0.8 m, the upper oil shale layer, up to 80 m thick, is generally uniform (Kasanin-Grubin, 1996; Kasanin-Grubin et al., 1997; Novkovic and Grgurovic, 1992). These organic rich sequences are characterized by thin lamination, preservation of plant leaves and absence of bioturbation, which requires permanent stratification of the water body and anoxic conditions (Obradovic et al., 1997). Bituminous marlstone deposited in a deeper lake facies (intrabasinal facies) form the uppermost unit of the Aleksinac series. It contains thin oil shale beds and (bituminous) marlstones interbedded with claystone and sandstone (Kasanin-Grubin et al., 1997). Warm and subtropic regimes changed with humid and dry periods during the deposition and diagenesis of the layers (Obradovic et al., 1997).

The organic and inorganic parts of the oil shales indicate that they were formed by algal blooms in the marginal part of a shallow, freshwater basin (Kasanin-Grubin et al., 1997). The lower oil shale layer has three seams of oil shale, an average net thickness of 25 m and a mean oil yield of 12.5 wt.%. The upper oil shale directly overlies the main coal seam and is referred to as "main level of oil shale". It contains the main productive shale with an average oil yield of 8.5 wt.% and has an average net thickness of 56 m, in the Dubrava Field up to 70 m (Ercegovac, 1990). At the end of the Early Miocene the deposit was divided into numerous blocks by intensive folding and faulting with significant horizontal and vertical movement. The general strike direction of oil shale is NNW-SSE and dip angles vary from 0°

(horizontal) to 90° (vertical) (Cokorilo et al., 2009). The structure of the basin fill is illustrated along profile D4 (Figure 2.5). In this sketch the sampled borhole BD-4 is right nearby of the illustrated borehole B-S 17. The inclination and deviation of B-S 17 is unknown. It hast to be mentioned that this sketch has been made before the borehole was drilled.

The projected drilling angle of well BD-4 was 57°. However variations of the angle between the core axis and oil shale laminations indicate that this deviation was not successfully maintained. The varying dipping angle of the oil shale layers resulted in an average drilling angle of ~50°. Figure 2.6 indicates true layer thicknesses (0 m – 214 m) which were calculated by an average correction multiplier of 0.75, meaning that 2 m of apparent thickness corresponds roughly to 1.5 m of the true thickness.

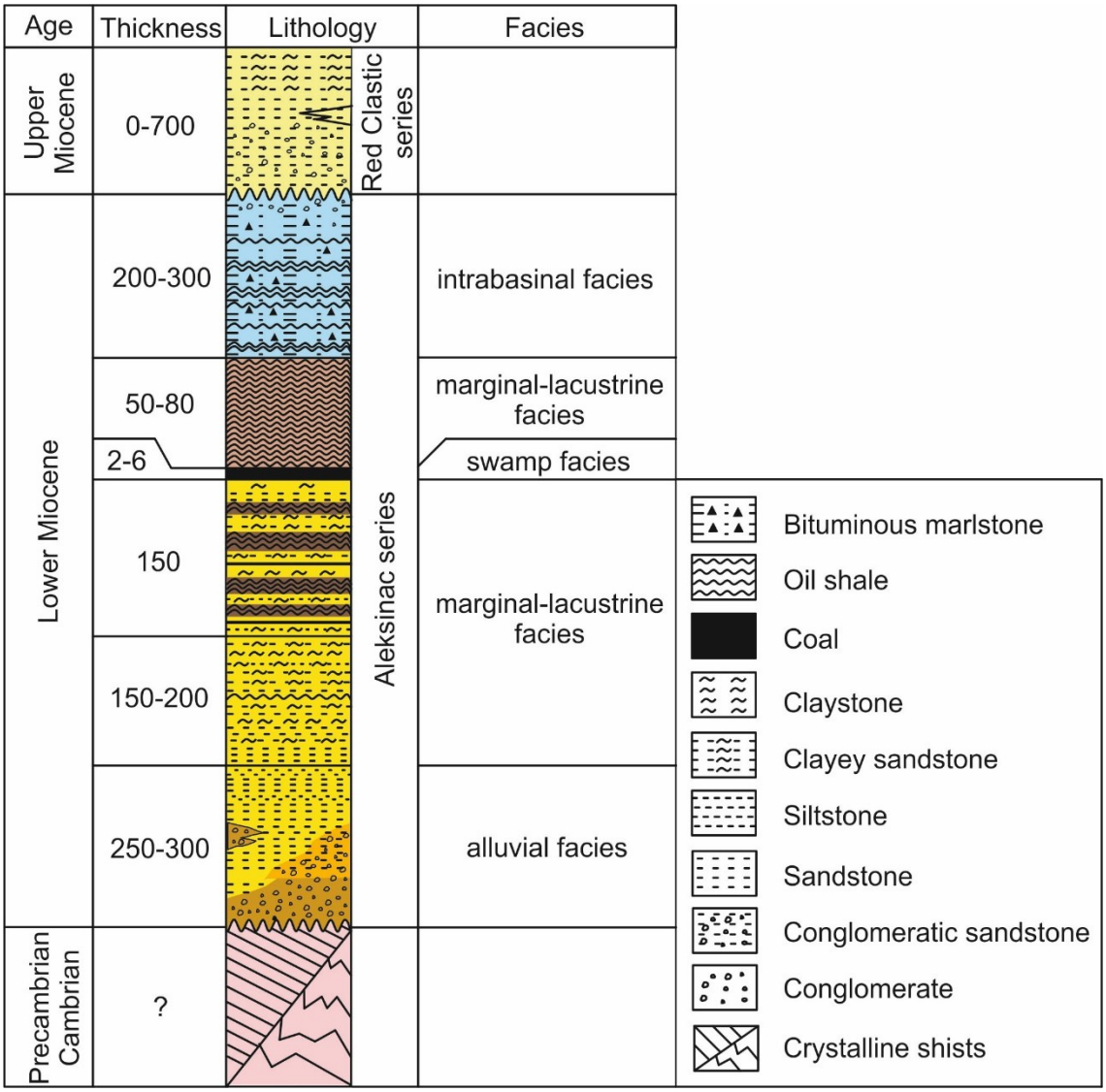

Figure 2.4: Stratigraphic column of the Aleksinac Basin (modified after Novkovic and Grgurovic, 1992)

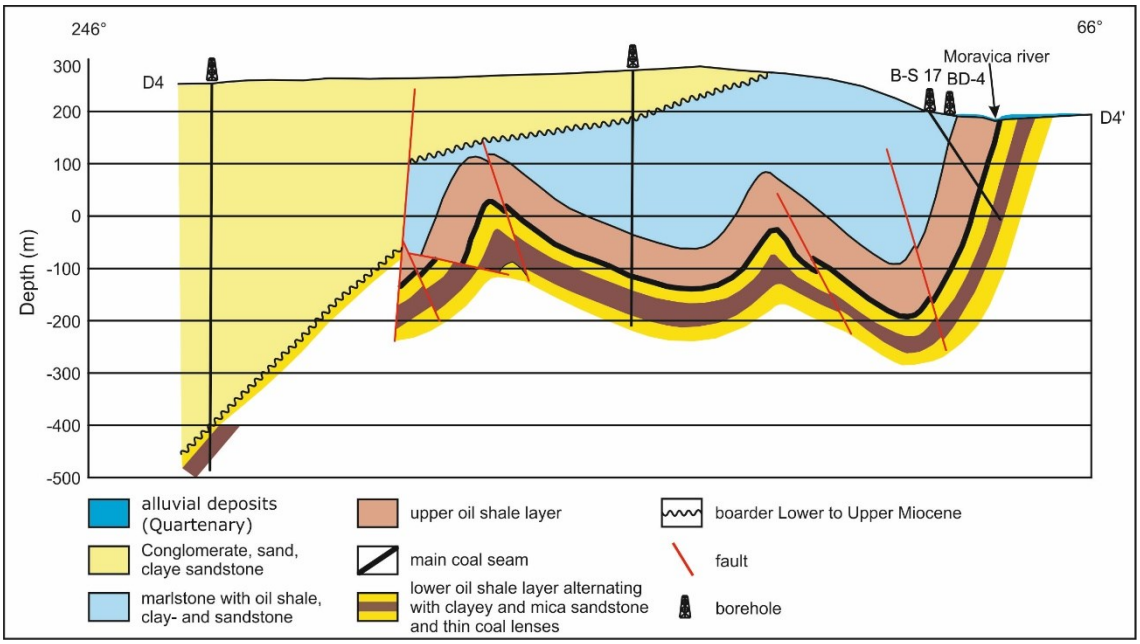

Figure 2.5: Sketch of the Aleksinac Basin along the geological profile D4-D4' marked in Figure 2.3 (modified after Cokorilo et al., 2009)

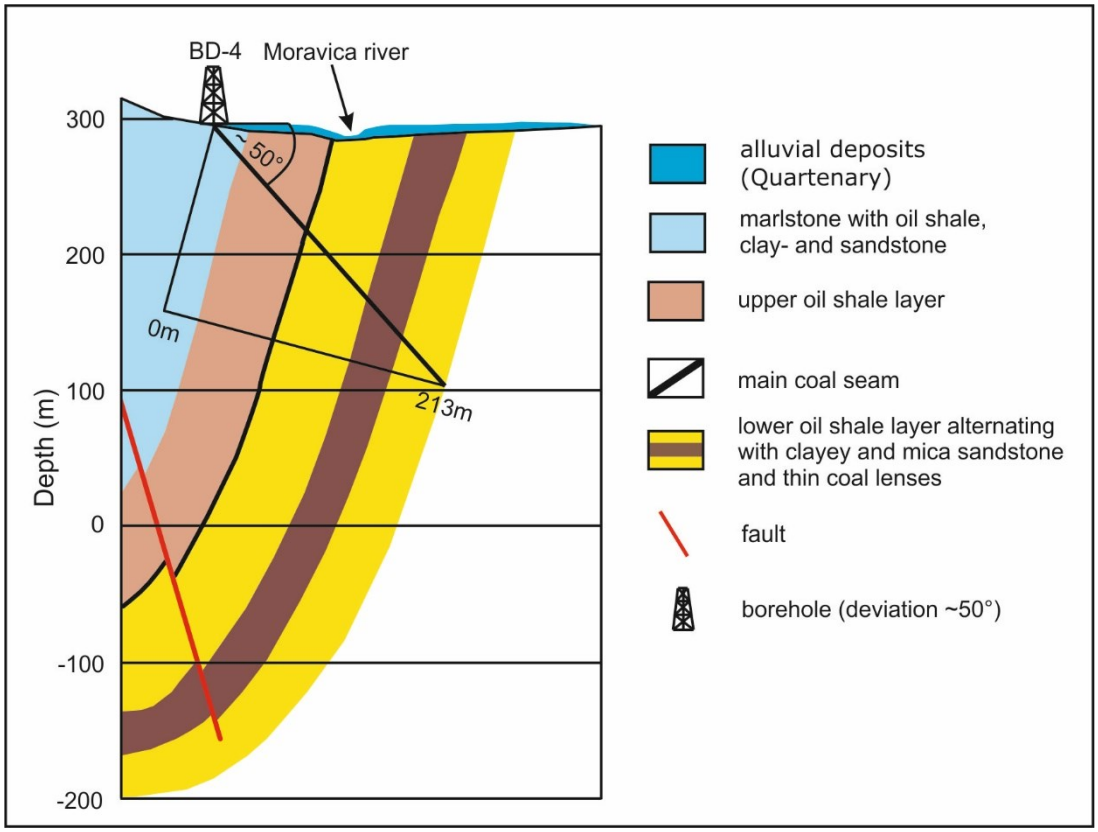

Figure 2.6: Sketch of the drilled borehole BD-4 (deviation ~50°) indicating true layer thicknesses (0 m – 213 m)

3. Samples and Methods

89 samples were collected by staff from the Faculty of Mining and Geology at the University of Belgrade (Serbia) from the deviated borehole BD-4/2011 drilled near the village of Subotinac in the Dubrava field, 9 km north of Aleksinac town (Figure 2.2). Most samples are typically representative for a core interval 2 m long, which corresponds roughly to 1.5 m of true thickness (e.g. Dub-05 at 28.0 m depth means, that 28.75 m is the base of this interval, 28.0 m is the centre of this interval and 27.25 is the top of this interval). Due to various but unknown reasons some samples represent lower or higher intervals (0.5 m or 2 m). The samples Dub-02 and Dub-01 represent thin layers of bituminous marlstones which are embedded in marly and clayey sandstones. All given depths represent true stratigraphic depth below the well top.

Representative portions of each sample were dried and powdered at the University of Belgrade. The samples were taken within a depth interval of 13 to 213 m and represents different lithologies (bituminous marlstone, oil shale, coal, sandstone, clay), but most samples are light grey to brown-grey oil shale samples and dark grey to black coaly samples. The samples were sent by Prof. Aleksandar Kostic (Faculty of Mining and Geology; University of Belgrade) to the Chair of Petroleum Geology (Montanuniversitaet Leoben, Austria) in summer 2016.

Within the frame of the present master´s thesis, the samples were analysed at the Chair of Petroleum Geology for organic geochemical and organic petrographical parameters. The following sections briefly explain the theory behind the applied analytical methods and the associated measurement procedures.

3.1 Elemental analysis (TC, S, TOC)

The effectiveness of a source rock is dependent on the quantity, quality, and maturity of the organic matter it contains (Peters et al., 2005b). For the present investigation an Eltra Helios Double Dual Range C/S Analyser was used to determine total amounts of carbon (TC) and sulphur (S), as well as total organic carbon (TOC). TOC content is a measure for the quantity of organic matter and therefore the organic richness of a rock sample. It provides a quick insight into the amount of hydrocarbons which can be generated and is therefore the first screening parameter used in source rock analysis. The difference between TC and TOC is the total inorganic carbon (TIC), which is derived from mineral matter. TIC contents were used to calculate calcite equivalent percentages ($calcite_{eq}$) with the equation $calcite_{eq}$ = TIC*8.34.

To determine the amount of TC and sulphur 80 to 100 mg of powdered sample was burnt at 1350°C in a pure oxygen atmosphere. Any present carbon and sulphur was converted to CO_2 and SO_2, which was quantified using an infra-red detection cell.

The mass of the released gases was converted to %C and %S based on the dry sample weight. Samples used for TOC measurements were pre-treated twice with distilled water followed by 50% phosphoric acid to carbonate minerals. Overnight they were dried on a heater at roughly 100°C and the same measuring process described above was carried out again to determine TOC content. Each sample was measured twice and a mean value for TC, TOC and S with the unit mass percent was calculated.

3.2 Rock Eval pyrolysis

Rock Eval pyrolysis enables determination of the generative potential, kerogen type and maturation stage of the samples. Pyrolysis was carried out using a "Rock Eval 6 classic" instrument (Vinci Technologies) in combination with the "Rockplus" Software. Dependent on the TOC content a predefined weight of each sample was analysed (higher TOC needs less sample weight). Each sample was measured in duplicate.

During the first stage of pyrolysis, the sample was heated up to 300°C in an inert helium atmosphere. After that, the temperature was kept constant for three minutes while free and adsorbed hydrocarbons were released and measured by a flame ionization detector (FID) to give the S_1 peak [mg HC/g rock]. In the second stage, the sample was heated gradually from 300 to 550°C at a rate of 25°C per minute. Through thermal cracking kerogen and heavy extractable compounds such as resins and asphaltenes were converted into hydrocarbons to give the S_2 peak [mg HC/g rock]. The temperature at which the maximum S_2 occurred was recorded as T_{max}. If T_{max} increases higher thermal energy is required to generate hydrocarbons from kerogen.

S_1 (free hydrocarbons) and S_2 (hydrocarbons generated during heating process) were used to calculate relevant parameters which are essential for the evaluation of hydrocarbon source potential. The hydrogen index (HI) indicates if a source rock is likely to be oil or gas prone (Table 3.1) and is calculated using the following equation (Espitalie et al., 1977):

$$\text{HI [mg HC/g TOC]} = \frac{S_2 \times 100}{\text{TOC}}$$

*Table 3.1: Source potential based on HI (Peters, 1986); *at peak maturity*

Kerogen Type	HI [mg HC/g TOC]	Expelled Product*
I	> 300	Oil
II	150-300	Oil/Gas
III	< 150	Gas

The sum of S_1 and S_2 gives the hydrocarbon generation potential. The production index (PI) gives information about the maturity of a source rock and is an indication of the amount of hydrocarbons which has been produced geologically relative to the total amount of hydrocarbons which the sample is able to produce (Espitalie et al., 1977):

$$PI = \frac{S_1}{S_1 + S_2}$$

The description of the source potential based on TOC and Rock Eval data follows Peters (1986, Table 3.2).

Table 3.2: Source potential based on TOC and S_2 (Peters, 1986)

Quality	**TOC** [%]	**S_2** [mg HC/g TOC]
poor	< 0.5	< 2.5
fair	0.5-1	2.5-5
good	1-2	5-10
very good	> 2	> 10

3.3 Vitrinite reflectance measurements

In addition to Rock Eval pyrolysis, another possibility for determining the thermal maturity of a sample is by measuring the reflectance of vitrinite macerals (Tissot and Welte, 1984; Mukhopadhyay and Dow, 1994). Vitrinite reflectance increases progressively with thermal maturation.

A Leica MPV microscope (100x magnification), equipped with an oil immersion objective, was used to determine random vitrinite reflectance (%R_r) of some polished blocks following established procedures (Taylor at al., 1998). The intensity of reflected light with a wavelength of 546nm was measured with a photomultiplier on at least 30 points per sample. For calibration an yttrium aluminium garnet standard (YAG, R_r = 0.899%) and a gadolinium gallium garnet standard (GGG, R_r = 1.699%) were used. The preparation of the polished blocks is explained in chapter 3.4. Table 3.3 summarizes the threshold values of three maturation parameters for the bottom and top of the oil window (Peters, 1986).

Table 3.3: Geochemical and optical parameters describing thermal maturation levels (Peters, 1986)

Maturity Level	**PI**	**T_{max}** [°C]	**R_r** [%]
Top of oil window	*~0.1*	*~435-445*	*~0.6*
Bottom of oil window	*~0.4*	*~470*	*~1.4*

3.4 Organic petrography

Attempts have been made to classify different types of oil shale on the basis of the depositional environment, the petrographic character of the organic matter, and the precursor organisms from which the organic matter was derived. A useful classification scheme for oil shales was developed by Hutton (1987, 1988, 1991), who came up with the idea that oil shales should be classified primarily based on the origin of the organic matter (terrestrial, lacustrine or marine). While terrestrial oil shales include resins, spores, waxy cuticles, corky tissue of roots, and stems of vascular terrestrial plants commonly found in coal-forming swamps and bogs, lacustrine oil shales mainly consist of algae that lived in freshwater, brackish or saline lakes. Marine oil shales are composed of marine algae or marine dinoflagellates. Organic petrography techniques enable the quantification of maceral percentages in oil shales on basis of maceral composition. Macerals are divided into three groups: (1) liptinite (algae, spores, cork, resin, cuticles), (2) vitrinite (higher plants) and (3) inertinite (burned plant tissues, charcoal).

For organic petrographical investigations 24 polished blocks of selected samples (chosen according to TOC content and position within the well) were prepared. The first step involved embedding of the crushed samples (grains ≤ 1.5 mm) in epoxy resin. Further on, grinding and polishing was done in seven steps using silicon carbide powder (graining: 220, 600, and 1200), diamond suspensions (9 µm, 3 µm, and 1 µm), and oxide polishing suspension colloidal silica (OPS; 0.05 µm). The presence of clay minerals forced the usage of ethylene glycol during the grinding and polishing procedure to avoid destruction of the sections.

The maceral composition was assessed semi-quantitatively with an incident light Leica MPV microscope using reflected white light and fluorescent light and oil immersion objectives (50x magnification). Around 1000 points per polished block were counted to get a significant amount of organic points.

3.5 Organic geochemistry (biomarker analyses)

Gas Chromatography-Mass Spectroscopy (GC-MS) is a method to obtain biomarker data from rock samples. This organic geochemical analysis followed procedures well established at the Chair of Petroleum Geology (Bechtel et al., 2012).

In a first step representative aliquots of 28 selected samples were extracted for approximately 1 h using dichloromethane (DCM) in a Dionex ASE 200 accelerated solvent extractor at 75°C and 50 bar. The extracts were then evaporated to 0.5 ml using a Zymark TurboVap 500 closed cell concentrator. Further on asphaltenes were precipitated from a hexane-DCM solution (80:1) and separated using centrifugation. The hexane-soluble fractions were separated into NSO compounds,

saturated hydrocarbons and aromatic hydrocarbons using medium pressure liquid chromatography (MPLC) with a Köhnen-Willsch instrument (Radke et al., 1980).

To obtain biomarker data the saturated and aromatic hydrocarbon fractions were analysed using a gas chromatograph equipped with a 60 m DB-5MS fused silica column and coupled to a Finnigan MAT GCQ ion trap mass spectrometer (GCeMS system). The oven temperature was programmed from 70 to 300°C at 4°C min^{-1}, followed by an isothermal period of 15 min. Helium was used as carrier gas. The sample was injected with an injector temperature of 275°C. The spectrometer was operated in the electron ionization (EI) mode over a mass/charge (m/z) scanning range between 50 and 650 with 0.7 s per scan.

The GC-MS data were processed in an Xcalibur data system. Individual components were identified on the basis of retention time in the total ion current (TIC) chromatogram and by comparison of the mass spectra with published data. Relative percentages and absolute concentrations of various compound groups in the aliphatic and aromatic hydrocarbon fractions were calculated using their peaks in TIC chromatograms and their relation to the peaks of the internal standards (1,1-binaphthyl). The concentrations were normalized to the TOC content.

3.6 Stable isotope geochemistry

For bulk carbon isotope analyses powdered samples were treated with hydrochloric acid to remove inorganic carbon. Decarbonated bulk rock samples and saturated and aromatic hydrocarbon fractions of rock extracts were placed into tin foil boats and combusted using an elemental analyser (Flash EA 1112) at 1020°C in an excess of oxygen. The resulting CO_2, separated by column chromatography, was analysed online by a ThermoFisher DELTA-V isotope ratio mass spectrometer. The $^{13}C/^{12}C$ isotope ratios of the CO_2 were compared with the corresponding ratio in a monitoring gas, calibrated against the Vienna-Pee Dee Belemnite (V-PDB) standard by the NBS-19 reference material. Stable isotope ratios are reported in delta notation ($\delta^{13}C$, Coplen, 2011) relative to the V-PDB standard ($\delta^{13}C = [(^{13}C/^{12}C)_{sample}/(^{13}C/^{12}C)_{standard} - 1]$). The reproducibility of the total analytical procedure is in the range of 0.1–0.2‰.

4. Results

4.1 Bulk geochemical parameters

Bulk geochemical parameters of the studied profile are listed in Table 4.1. Vertical profiles of calcite$_{equ}$, TOC, HI, T_{max}, S and TOC/S based on elemental analyses and Rock Eval pyrolysis data are shown in Figure 4.1. Also the vertical variation of $\delta^{13}C$ of total organic matter and maceral composition is indicated in Figure 4.1. The red dots symbolise the samples which were analysed according to organic petrography and organic geochemistry.

Table 4.1: Bulk geochemical data (Eltra, Rock-Eval) of sediments in the Aleksinac Basin

Sample	Depth (m)	Calcite$_{equ}$ (wt.%)	TOC (wt.%)	S (wt.%)	TOC/S	S_1 (mgHC/g)	S_2 (mgHC/g)	S_1+S_2 (mgHC/g)	PI	T_{max} (°C)	HI (mgHC/gTOC)
Bituminous marlstone											
Dub-01	13,00	22,6	6,4	0,3	18,63	0,8	55,7	56,5	0,01	435	875
Dub-02	17,00	36,0	6,2	0,4	17,29	0,7	54,6	55,3	0,01	439	881
Dub-03	23,50	43,6	13,1	2,9	4,45	1,3	107,3	108,5	0,01	438	818
Upper oil shale layer											
Dub-04	26,50	39,2	18,5	3,6	5,16	1,9	156,2	158,1	0,01	436	843
Dub-05	28,00	23,4	19,8	3,7	5,32	2,1	169,7	171,8	0,01	439	856
Dub-06	29,50	28,5	16,6	3,3	4,98	1,4	144,7	146,1	0,01	438	870
Dub-07	31,00	31,6	16,8	3,4	4,93	1,6	146,5	148,1	0,01	439	874
Dub-08	32,50	31,2	21,9	3,2	6,92	2,7	196,0	198,7	0,01	437	897
Dub-09	34,00	30,7	11,0	2,1	5,26	1,0	97,2	98,2	0,01	439	881
Dub-10	35,50	28,4	18,5	2,1	8,74	1,5	136,1	137,6	0,01	443	734
Dub-11	37,00	28,9	20,7	3,5	5,96	2,1	160,4	162,4	0,01	442	775
Dub-12	38,50	15,0	41,9	5,3	7,87	3,9	255,9	259,8	0,02	441	610
Dub-13	40,00	23,6	22,9	4,3	5,31	2,9	191,7	194,6	0,01	445	836
Dub-14	41,50	36,7	28,2	4,2	6,76	2,8	189,8	192,7	0,01	440	674
Dub-15	43,00	0,4	25,3	2,8	8,94	1,9	150,7	152,6	0,01	442	596
Dub-16	44,50	9,6	31,5	3,4	9,32	4,1	203,4	207,5	0,02	441	646
Dub-17	46,00	4,2	28,3	2,9	9,61	2,9	190,9	193,7	0,01	440	675
Dub-18	47,50	23,6	16,2	2,5	6,51	1,5	117,6	119,1	0,01	439	725
Dub-19	49,00	30,4	22,2	2,2	9,91	1,9	179,4	181,3	0,01	443	807
Dub-20	50,50	8,8	27,3	2,9	9,50	2,1	224,9	227,1	0,01	441	824
Dub-21	52,00	17,2	11,8	2,9	4,10	1,3	96,6	97,9	0,01	443	816
Dub-22	53,50	33,8	11,6	2,2	5,34	1,1	91,8	92,9	0,01	439	791
Dub-23	55,00	20,9	11,6	2,6	4,42	1,0	88,5	89,5	0,01	437	760
Dub-24	56,50	16,9	11,5	3,2	3,65	0,7	79,3	80,0	0,01	434	689
Dub-25	58,00	13,2	8,8	2,4	3,63	0,5	60,7	61,3	0,01	436	690
Dub-26	58,50	28,3	11,2	3,0	3,73	0,8	83,1	83,9	0,01	436	744
Dub-27	60,00	21,8	8,5	3,1	2,71	0,7	60,9	61,5	0,01	436	720
Dub-28	61,50	21,6	8,5	3,1	2,73	0,6	61,5	62,1	0,01	436	726
Dub-29	63,00	16,1	10,2	2,9	3,58	0,3	61,4	61,8	0,01	437	599
Dub-30	64,50	13,6	3,2	1,2	2,75	0,4	14,2	14,7	0,03	432	440
Dub-31	66,00	20,0	4,0	1,3	2,97	0,6	23,2	23,8	0,03	433	586
Dub-32	67,50	10,1	9,2	2,4	3,90	1,0	70,8	71,8	0,01	441	768
Dub-33	69,00	20,1	13,4	2,6	5,24	0,9	118,7	119,6	0,01	441	886
Dub-34	70,50	18,5	10,6	3,8	2,80	1,0	85,7	86,7	0,01	438	809
Dub-35	72,00	23,0	8,5	1,9	4,59	0,8	68,7	69,5	0,01	439	808
Dub-36	73,50	16,1	5,1	1,8	2,82	0,6	39,1	39,6	0,01	436	772
Dub-37	75,00	13,7	8,2	2,1	3,89	0,9	66,4	67,3	0,01	437	810
Dub-38	76,50	14,9	19,1	2,9	6,51	1,4	136,2	137,6	0,01	445	715
Dub-39	78,00	18,3	10,7	2,7	3,95	0,8	78,9	79,7	0,01	441	736
Dub-40	79,00	28,0	7,0	2,6	2,70	0,6	48,0	48,5	0,01	438	683
Dub-41	80,00	31,2	7,0	2,9	2,45	0,6	50,9	51,5	0,01	430	723
Dub-42	81,00	44,6	12,4	3,3	3,73	0,9	87,7	88,6	0,01	434	708
Dub-43	83,00	28,4	7,3	2,5	2,95	0,8	57,0	57,8	0,01	434	777
Dub-44	84,50	18,5	7,9	1,3	6,25	0,5	50,1	50,6	0,01	435	638
Dub-45	86,00	5,2	25,3	1,6	16,04	0,9	175,5	176,4	0,00	443	694
Main coal seam											
Dub-46	87,50	5,9	32,4	6,6	4,87	1,2	172,0	173,2	0,01	431	531
Dub-47	89,00	4,8	51,6	7,5	6,85	3,9	258,0	261,9	0,01	430	500
Dub-48	90,50	1,9	63,1	3,7	17,10	0,4	73,2	73,5	0,01	414	116

calcite$_{equ}$: calcite equivalent; TOC: total organic carbon; S: sulphur; S_1: free hydrocarbons; S_2: hydrocarbons generated during Rock-Eval pyrolysis
PI: production index; T_{max}: temperature of maximum hydrocarbon generation; HI: hydrogen index

Table 4.1 continued

Sample	Depth (m)	$Calcite_{equ}$ (wt.%)	TOC (wt.%)	S (wt.%)	TOC/S	S_1 (mgHC/g)	S_2 (mgHC/g)	S_1+S_2 (mgHC/g)	PI	T_{max} (°C)	HI (mgHC/gTOC)
Sandstone and clay											
Dub-49	95,00	0,2	2,30	0,72	3,18	0,1	3,1	3,2	0,04	429	134
Dub-50	130,00	1,3	9,07	8,52	1,06	0,1	5,1	5,3	0,03	416	56
Dub-51	140,00	4,7	8,68	2,54	3,42	0,2	13,8	14,0	0,01	433	159
Dub-52	141,50	2,2	2,44	1,24	1,97	0,1	3,7	3,8	0,02	436	153
Dub-53	143,00	1,7	8,15	2,25	3,62	0,1	5,3	5,4	0,02	429	65
Dub-54	144,50	1,4	2,15	1,90	1,13	0,0	0,9	1,0	0,04	431	44
Lower oil shale layer											
Dub-55	146,00	2,0	6,96	0,74	9,38	0,4	44,9	45,4	0,01	439	645
Dub-56	147,50	5,5	11,47	1,67	6,89	0,7	93,6	94,3	0,01	445	815
Dub-58	150,50	7,0	36,00	7,40	4,87	2,1	276,8	278,9	0,01	439	769
Dub-59	152,00	18,2	27,29	5,86	4,66	1,9	211,7	213,6	0,01	442	776
Dub-60	153,50	11,8	16,77	4,89	3,43	0,7	122,9	123,6	0,01	442	733
Dub-61	155,00	33,5	9,48	3,36	2,82	0,4	74,0	74,4	0,01	442	781
Dub-62	156,50	14,2	14,98	4,94	3,03	0,8	118,7	119,4	0,01	440	792
Dub-63	158,00	21,0	20,86	5,94	3,51	1,0	154,9	156,0	0,01	439	743
Dub-64	159,50	23,1	9,32	2,94	3,17	0,4	73,1	73,4	0,00	441	784
Dub-65	161,00	7,1	2,73	0,30	9,14	0,1	2,7	2,7	0,02	434	98
Dub-66	162,50	3,6	14,45	11,10	1,30	1,0	49,8	50,8	0,02	429	345
Dub-67	164,00	31,7	17,30	1,78	9,74	0,5	131,8	132,2	0,00	444	762
Dub-68	165,50	8,7	34,62	8,51	4,07	0,9	227,9	228,8	0,00	439	658
Dub-69	167,00	12,3	34,16	5,72	5,97	1,0	185,3	186,2	0,01	439	542
Dub-70	168,50	0,1	41,21	5,48	7,52	0,7	157,0	157,7	0,00	434	381
Dub-71	170,00	13,4	28,06	7,38	3,80	1,3	156,3	157,6	0,01	432	557
Dub-72	171,50	11,3	37,23	5,30	7,03	1,9	229,6	231,5	0,01	432	617
Dub-73	173,00	20,9	5,04	1,78	2,83	0,1	27,0	27,1	0,00	440	535
Dub-74	174,50	14,2	21,38	7,50	2,85	0,6	114,7	115,3	0,01	433	536
Dub-75	176,00	15,0	8,20	3,20	2,56	0,2	47,0	47,1	0,00	437	573
Sandstone interbedded with oil shale and coal lenses											
Dub-76	192,50	17,0	28,11	4,33	6,49	0,8	118,3	119,1	0,01	435	421
Dub-77	194,00	10,8	46,52	6,10	7,63	0,5	75,2	75,7	0,01	428	162
Dub-78	195,50	4,3	13,21	9,04	1,46	0,2	9,8	9,9	0,02	412	74
Dub-79	197,00	8,8	14,91	5,14	2,90	0,1	10,5	10,6	0,01	419	70
Dub-80	198,50	0,1	2,80	1,37	2,04	0,0	4,6	4,7	0,01	439	166
Dub-81	200,00	1,4	1,01	3,96	0,25	0,0	0,4	0,4	0,06	432	38
Dub-82	201,50	0,1	5,54	3,89	1,43	0,2	16,3	16,4	0,01	427	293
Dub-83	203,00	0,2	1,35	1,39	0,97	0,0	0,7	0,7	0,04	433	50
Dub-84	204,50	13,4	1,06	0,96	1,10	0,0	0,5	0,5	0,03	438	43
Dub-85	206,00	4,2	0,54	0,32	1,69	0,0	0,5	0,5	0,04	439	95
Dub-86	208,50	0,5	3,22	1,06	3,03	0,1	11,1	11,2	0,01	440	346
Dub-87	210,00	0,8	5,38	3,54	1,52	0,1	28,1	28,3	0,01	436	523
Dub-89	213,00	0,2	2,34	2,28	1,03	0,0	0,6	0,6	0,04	432	26

$calcite_{equ}$: calcite equivalent; TOC: total organic carbon; S: sulphur; S_1: free hydrocarbons; S_2: hydrocarbons generated during Rock-Eval pyrolysis
PI: production index; T_{max}: temperature of maximum hydrocarbon generation; HI: hydrogen index

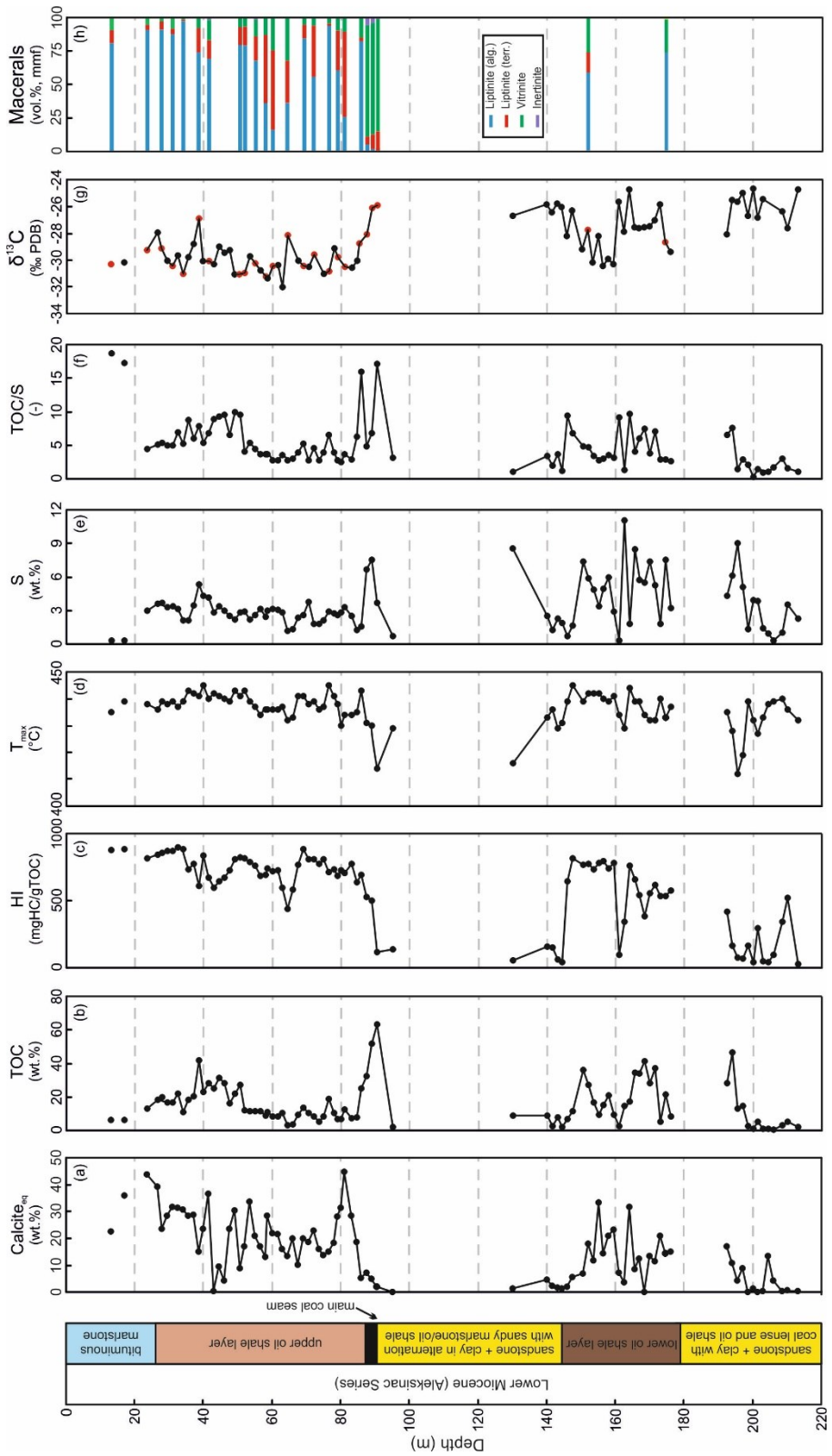

Figure 4.1: Stratigraphy and depth plot of bulk geochemical parameters; Calcite$_{equ}$: (a) calcite equivalent, (b) TOC: total organic carbon, (c) HI: hydrogen index, (d) T$_{max}$: temperature of maximum hydrocarbon generation, (e) S: sulphur, (f) TOC/S ratio, (g) δ^{13}C: carbon isotopic composition of organic matter, (h) maceral composition on a mineral matter free (mmf) basis

Calcite equivalent percentages ($calcite_{equ}$) in layers below the main coal seam are typically between 0 and 20 wt.% and tend to be lower than in samples overlying the coal seam. In the coal seam carbonate contents are around 5 wt.% and rise in the lowermost 7-m-thick interval of the upper oil shale layer to a maximum of 45 wt.% (Dub-42). Most samples in the upper oil shale layer show $calcite_{equ}$ percentages between 10 and 30 wt.%, following no clear trend. Samples representing bituminous marlstones show enhanced $calcite_{equ}$ varying between 22 and 44 wt.%.

Due to the alternation of sandy clay, oil shale and thin coal seams in the layers below the main coal seam no general trend of TOC contents can be determined. The TOC content of the main coal seam is high (up to 63 wt.%) and decreases gradually upwards. With the exception of the lowermost sample (25.3 wt.% TOC), TOC content in the lower part of the upper oil shale layer (86-52 m) typically is about 10 wt.%. TOC contents in the upper part (52-26 m) are higher and reach 42 wt.% in sample Dub-12 at 38.5 m. Samples representing bituminous marlstones show TOC contents between 6 and 13 wt.%.

Attributed to the different sediments in the layers below the main coal seam there is no specific trend of sulphur contents and TOC/S ratios in these layers. However, it is remarkable that sulphur contents in organic matter-rich rocks (>9.0 wt.% TOC) is typically higher (up to 14.4 wt.%) than in samples from the upper oil shale layer. In the coal seam the TOC/S ratio rises significantly to a value of 17 (Dub-48). Samples Dub-47 and Dub-46 show high sulphur contents (~7 wt.%) which results, despite of a high TOC content, in a relatively low TOC/S ratio. In the upper oil shale layer sulphur contents are more or less around 3 wt.%. Enhanced TOC contents from 52 m upwards lead to increasing TOC/S ratios above this depth. Ratios increase from values between 5 and 10 to values over 10. The uppermost two samples in the bituminous marlstone layer show low sulphur contents (<0.5 wt.%). As a result, TOC/S ratios in these samples are very high (>15).

Below the main coal seam hydrogen index (HI) values range from 30 to 800 mgHC/gTOC, depending on sandy clay, oil shale or coal. The HI of sample Dub-48 from the base of the main coal seam is 116 mgHC/gTOC. Significantly higher HI values (~500 mgHC/gTOC) are observed in the upper two samples of the main coal seam. A general upward increasing trend of the HI in the lower part of the upper oil shale layer (86 - 69 m) is observed. At around 64 m depth, HI declines to 440 mgHC/gTOC. Above this depth HI increases again and varies between 600 and 900 mgHC/gTOC with highest values from 34 m upwards.

Below the coal seam T_{max} follows the increasing and decreasing trend of the HI in a range from 412 to 445°C. This shows that T_{max} values are strongly controlled by kerogen type. In Dub-48 T_{max} declines to 414°C and increases in the other two samples of the main coal seam to 431°C. In the upper oil shale layer and bituminous marlstones T_{max} varies between 435 and 445°C. T_{max} values determined in coaly rocks indicate that the organic matter is thermally immature.

A plot of HI against T_{max} is shown in Figure 4.2. The plot shows that samples from the lower oil shale layer represent type I and type II kerogen (oil prone). Nearly all samples of the upper oil shale layer represent type I kerogen (highly oil prone). Type III kerogen is present in sandstones, siltstones, clays and coal samples. However, based on high HI values, the organic matter in two samples from the main coal seam has to be classified as type II kerogen.

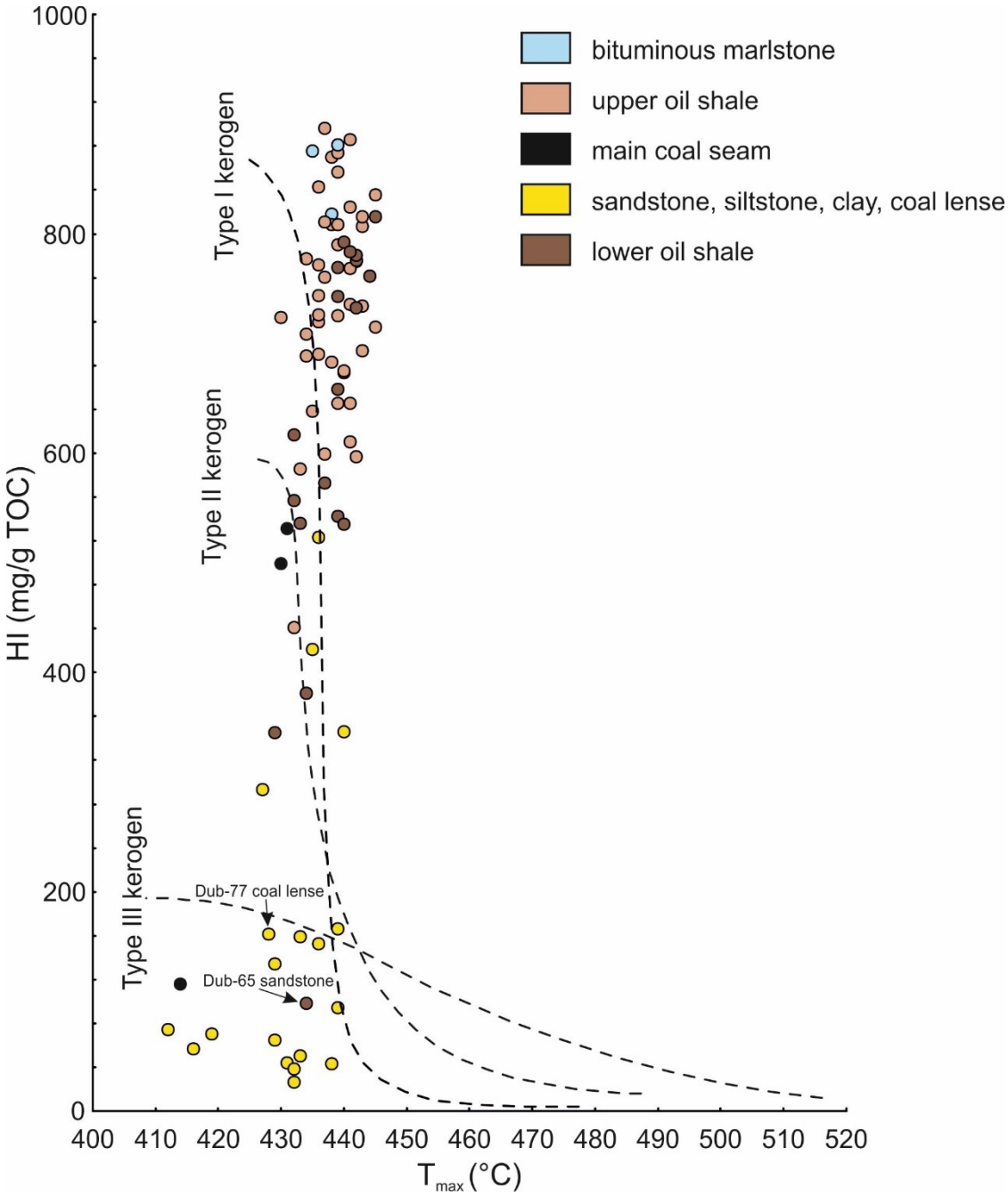

Figure 4.2: Plot of Hydrogen Index (HI) versus T_{max} (according to Espitalie et al, 1984) outlining the kerogen-type of different layers in the Aleksinac series

Due to the potential presence of faults, the layers below the main coal seam are characterized by an unclear stratigraphy. For organic petrographical and organic geochemical investigations most of the analysed samples were picked from the uniform upper oil shale and the main coal seam. Therefore, in the following two chapters the obtained results are presented from top to base and not as before from base to top.

4.2 Organic petrography and vitrinite reflectance

24 organic matter-rich samples were selected for organic petrological investigations. Maceral percentages are listed in Table 4.2. In this table percentages of mineral matrix (clay minerals, quartz, dolomite, calcite, etc.), pyrite, liptinite of algal (liptinite alg.) and terrigenous origin (liptinite terr.), vitrinite and inertinite are distinguished. In additional columns, percentages of total organic matter (Σ OM) as well as maceral percentages on a mineral matter free (mmf) basis are shown. Maceral percentages on mmf basis are also displayed in Figure 4.1h. Considering the sum of organic matter in Table 4.2, a downward decrease at around 52 m is obvious.

Table 4.2: Data from elemental analysis, Rock Eval pyrolysis and organic petrographical investigations

Sample	Depth (m)	TOC (wt.%)	S (wt.%)	HI (mgHC/gTOC)	Mineral Matrix (vol.%)	Pyrite (vol.%)	Liptinite (alg.) Lamalginite (vol.%)	Liptinite (alg.) Telalginite (vol.%)	Liptinite (terr.) Sporinite (vol.%)	Liptinite (terr.) Cutinite (vol.%)	Liptinite (terr.) Fluorinite (vol.%)	**Vitrinite** (vol.%)	**Inertinite** (vol.%)	**Σ OM** (vol.%)	Liptinite (alg.) (vol. % mmf)	Liptinite (terr.) (vol. % mmf)	Vitrinite (vol. % mmf)	Inertinite (vol. % mmf)
Bituminous marlstone																		
Dub-01	13.0	6.36	0.34	875	91.3	0.5	6.6		0.2	0.6		0.7	0.0	8.2	81.3	9.9	8.8	0.0
Dub-03	23.5	13.11	2.95	818	75.6	3.4	17.6	1.6	0.2	0.6		1.0	0.0	21.0	91.4	3.8	4.8	0.0
Upper oil shale layer																		
Dub-05	28.0	19.81	3.72	856	72.2	4.4	20.4	1.0	1.5			0.5	0.0	23.4	91.6	6.3	2.1	0.0
Dub-07	31.0	16.77	3.40	874	75.4	3.9	17.4	0.9	0.5	0.3		1.6	0.0	20.7	88.1	4.2	7.7	0.0
Dub-09	34.0	11.03	2.10	881	82.1	3.1	14.4	0.1	0.1			0.1	0.0	14.9	98.0	1.0	1.0	0.0
Dub-12	38.5	41.93	5.33	610	49.6	5.9	32.8	0.3	7.5	0.7		3.2	0.0	44.5	74.4	18.3	7.3	0.0
Dub-14	41.5	28.18	4.17	674	62.6	4.8	21.9	0.8	3.8	0.8		5.0	0.4	32.7	69.5	14.0	15.2	1.2
Dub-20	50.5	27.30	2.87	824	63.8	3.6	25.7	0.4	4.4			2.2	0.0	32.7	80.0	13.3	6.7	0.0
Dub-21	52.0	11.85	2.89	816	80.2	3.5	13.0		2.2	0.1		1.0	0.0	16.3	79.6	14.2	6.2	0.0
Dub-23	55.0	11.64	2.63	760	81.1	2.9	10.7	0.2	2.9			2.0	0.2	16.0	68.3	18.3	12.5	1.0
Dub-25	58.0	8.80	2.42	690	85.0	3.4	4.2		6.0			1.4	0.0	11.6	36.2	51.4	12.4	0.0
Dub-27	60.0	8.46	3.12	720	83.6	4.0	2.0		7.5			3.0	0.0	12.4	16.0	60.0	24.0	0.0
Dub-30	64.5	3.23	1.18	440	91.3	2.3	2.3		2.0			2.0	0.0	6.4	36.4	31.8	31.8	0.0
Dub-33	69.0	13.40	2.56	886	79.3	3.4	13.1	1.6	1.8			0.8	0.0	17.3	84.9	10.4	4.7	0.0
Dub-35	72.0	8.50	1.85	808	86.8	2.9	4.5	1.3	4.0			0.6	0.0	10.3	55.8	38.8	5.4	0.0
Dub-38	76.5	19.05	2.93	715	74.3	3.9	20.5		0.4			0.8	0.0	21.8	94.3	1.9	3.8	0.0
Dub-40	79.0	7.03	2.61	683	87.6	3.2	5.2	0.4	2.8			0.8	0.0	9.3	60.6	30.3	9.1	0.0
Dub-42	81.0	12.37	3.32	708	82.5	3.7	3.3	0.2	8.9			1.4	0.0	13.8	25.7	64.3	10.0	0.0
Dub-45	86.0	25.30	1.58	694	67.2	2.5	23.5	1.7	0.8			4.4	0.0	30.4	82.9	2.7	14.4	0.0
Main coal seam																		
Dub-46	87.5	32.36	6.65	531	55.4	8.5	1.2	0.7	1.7		0.3	30.6	1.9	36.1	5.3	5.6	83.9	5.3
Dub-47	89.0	51.64	7.54	500	44.2	9.0		0.7	2.0	3.0	0.3	39.5	1.7	46.9	1.5	11.3	83.7	3.6
Dub-48	90.5	63.08	3.69	116	25.5	3.9			3.3	5.7	1.5	59.6	0.5	70.7	0.0	15.2	84.0	0.7
Lower oil shale layer																		
Dub-59	152.0	27.29	5.86	776	66.0	6.3	15.4	1.1	4.2			7.0	0.0	27.7	59.5	15.2	25.3	0.0
Dub-74	174.5	21.38	7.50	536	62.8	9.3	20.0	0.8				6.9	0.2	27.9	74.6	0.0	24.7	0.7

Liptinite of algal origin dominates down to 52 m (79-98 vol.% mmf). In these layers lamalginite is the most abundant liptinite maceral. Telalginite occurs in minor amounts within this section. Telalginite is derived from large colonial or thick-walled unicellular algae, typified by genera such as Botryococcus, found in fresh- and brackish water lakes. Lamalginite includes thin-walled colonial or unicellular algae (Dyni, 2005). While telalginite is typically characterized by a greenish fluorescence colour, lamalginite displays yellow to orange colours under fluorescent light (Figure 4.3f).

Although lamalginite is mostly dominating also below 52 m depth, the input of terrigenous organic matter rises. Sporinite as the predominant landplant derived terrigenous liptinite maceral as well as vitrinite appear below this depth in higher abundances. Typically vitrinite particles are small. Inertinite is largely absent in all layers above the main coal seam (< 1.2 vol.% mmf). In the upper oil shale layer samples show an average vitrinite reflectance of 0.44%R_r (average standard deviation: 0.0218). This average value results from the samples Dub-5, Dub-12, Dub-27, Dub-40, Dub-42 and Dub-45. Framboidal pyrite is common in all samples, but especially abundant in samples from the lower oil shale layer and from the main coal seam.

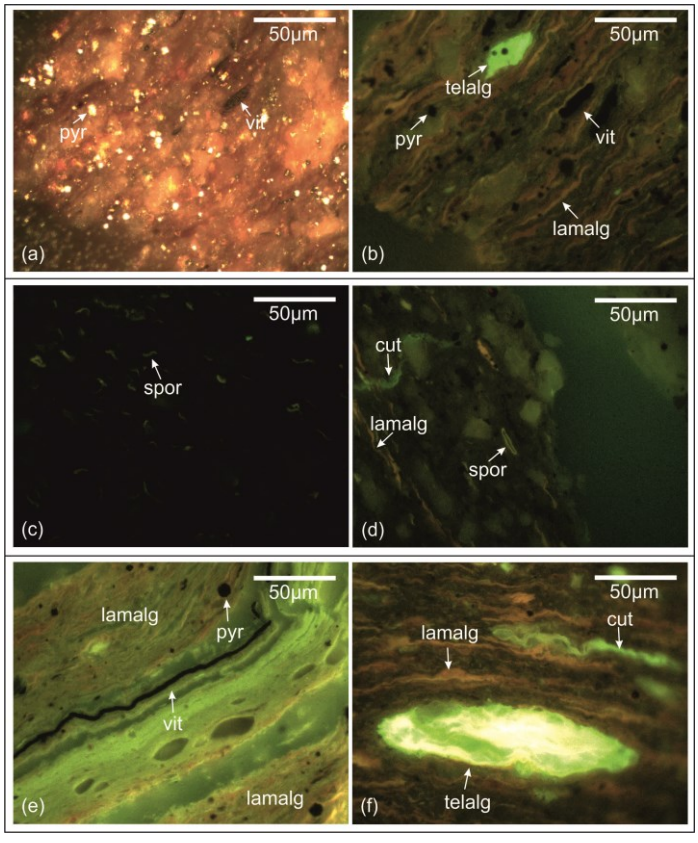

Figure 4.3: Microphotographs of samples from the upper oil shale layer: (a) Dub-05 under white light, (b) Dub-05 under UV light, (c) Dub-25 under UV light, (d) Dub-40 under UV light, (e) Dub-38 under UV light, (f) Dub-45 under UV light. pyr: pyrite, vit: vitrinite, telalg: telalginite, lamalg: lamalginite, spor: sporinite, cut: cutinite

Vitrinite is the major maceral group in samples from the coal seam (~84 vol.% mmf). Vitrodetrinite is the prevailing vitrinite maceral, whereas corpogelinite is rare. The vitrinite particles are much bigger than in the upper oil shale layer. Algal liptinite (<6 vol.% mmf) in form of lamalginite and telalginite, as well as terrigenous liptinite (5-15 vol.% mmf) represented by sporinite, cutinite and fluorinite occur in minor amounts. Inertinite is present up to 5 vol.% mmf. Funginite as an example for an inertinite maceral is visible in Figure 4.4c,d. The cavities of the funginite particle are filled by migrated bitumen (exsudatinite) with an orange fluorescence colour, formed during early oil generation. Average vitrinite reflectance, both in Dub-46 and Dub-47, is 0.52%R_r (average standard deviation: 0.0331). Sample Dub-48 shows a vitrinite reflectance of 0.56%R_r (standard deviation: 0.0234). Vitrtinite reflectance was measured on vitrodetrinite particles. Corpogelinite show obvious higher vitrinite reflectance than vitrodetrinite.

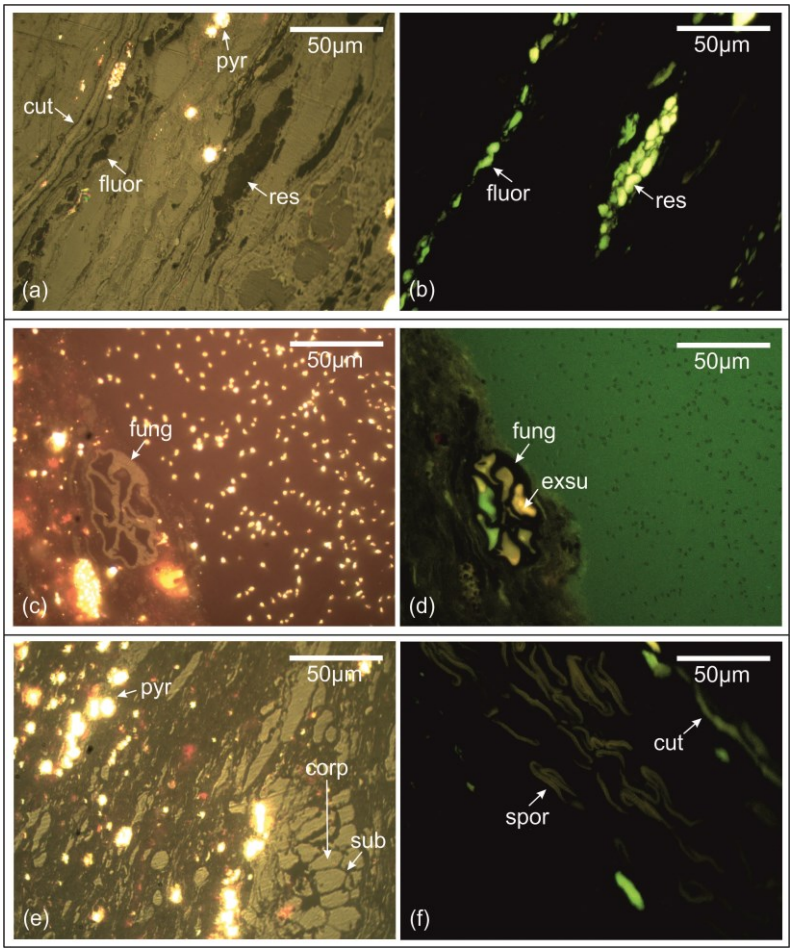

Figure 4.4: Microphotographs of samples from the main coal seam: (a) Dub-48 under white light, (b) Dub-48 under UV light, (c) Dub-47 under white light, (d) Dub-47 under UV light, (e) Dub-47 under white light, (f) Dub-48 under UV light. pyr: pyrite, fluor: fluorinite, spor: sporinite, cut: cutinite, res: resinite, fung: funginite, exsu: exsudatinite, corp: corpogelinite, sub: suberinite

Additional microphotographs of samples from the upper oil shale layer and the main coal seam are visible in the Appendix.

For comparison, two samples from the lower oil shale layer (under the main coal seam) were analysed. Again, lamalginite is dominating in both samples (60 and 75 vol.%). Terrigenous organic matter constitutes between 25 and 40 vol.% and is represented by sporinite and vitrinite.

Cross plots of sulphur content and pyrite percentages, TOC content and the sum of organic matter (Σ OM) as well as between HI and liptinite are shown in Figure 4.5 and can be used for a simple quality check. As expected, there is an excellent correlation between sulphur content and pyrite percentages (r^2=0.97) and between TOC content and Σ OM (r^2=0.97). There is a moderate correlation between liptinite percentages (liptinite alg. + liptinite terr., mmf) and HI (r^2=0.61) for non-coal samples. Two coal samples with relative low liptinite percentages are characterized by high HI values (~500 mgHC/gTOC). This may be due to the presence of bitumen-impregnated vitrinite.

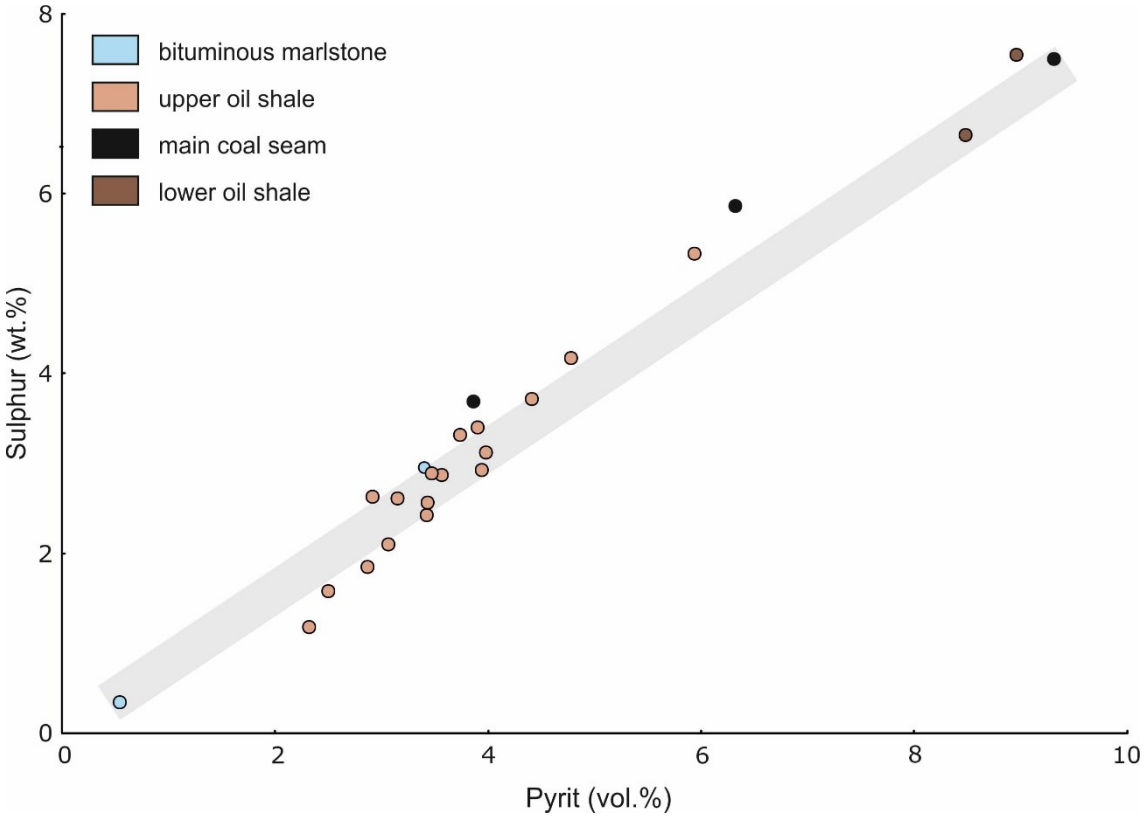

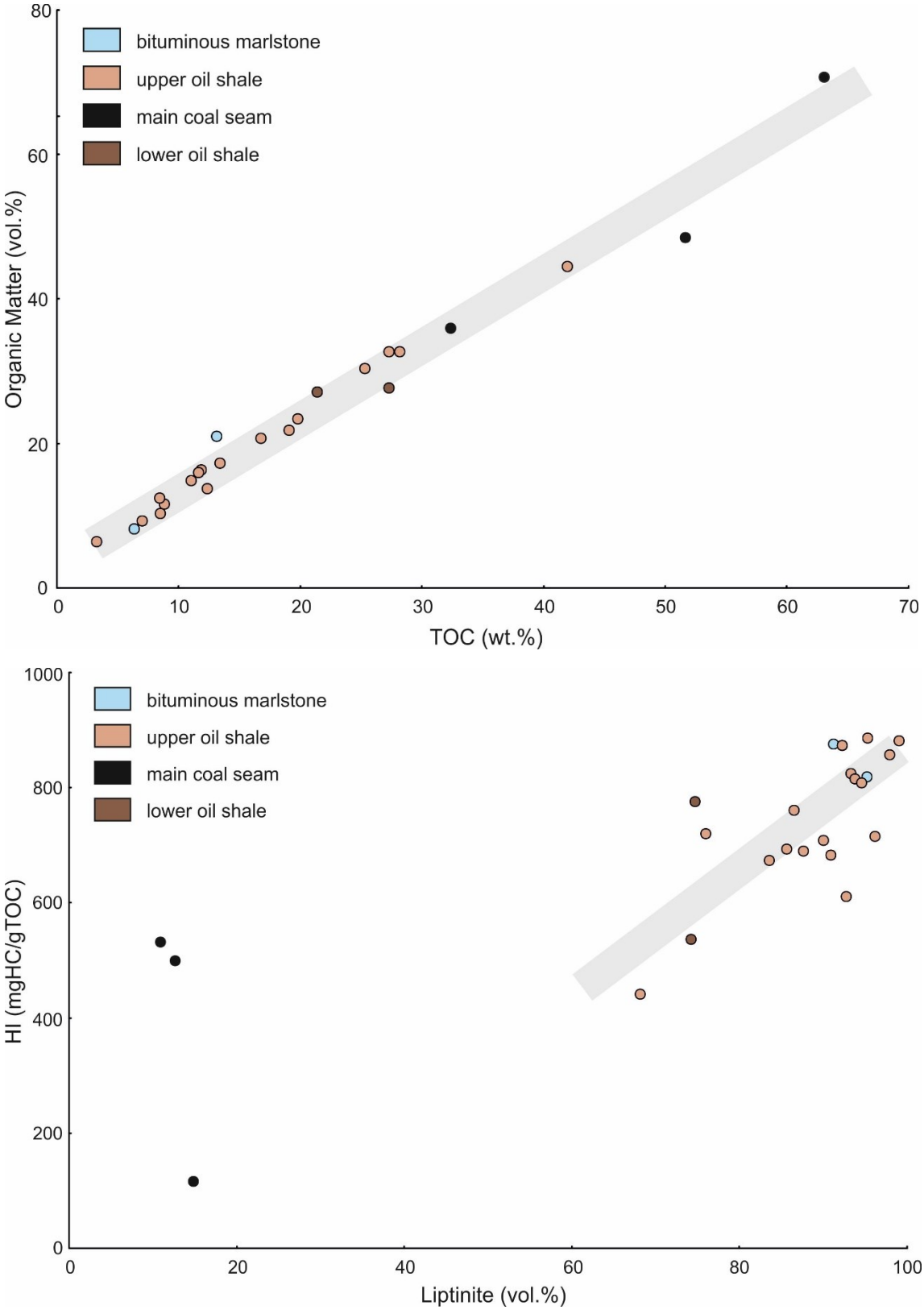

Figure 4.5: Bulk and Rock-Eval parameters plotted versus organic petrological parameters. Note high HI values of two coal samples despite of low liptinite contents.

4.3 Organic geochemistry

28 samples were selected for organic geochemical investigations. Concentrations and concentration ratios in the hydrocarbon fractions are listed in Table 4.3.

Table 4.3: Data from biomarker analysis

Sample	Depth	TOC	EOM	Sat. HC	Aro. HC	NSO	Asphalt.	n-alk.	n-$C_{15\text{-}19}$ / n-alk.	n-$C_{21\text{-}25}$ / n-alk.	n-$C_{27\text{-}31}$ / n-alk.	CPI	Pr/Ph	Pr/n-C_{17}	Ph/n-C_{18}
	(m)	(wt.%)	(mg/g TOC)	(%)	(%)	(%)	(%)	(µg/gTOC)							
Bituminous marlstone															
Dub-01	13.0	6.4	43.3	17	4	51	27	418	0.16	0.48	0.28	3.9	0.23	2.37	7.99
Dub-02	17.0	6.2	23.8	26	7	57	9	801	0.08	0.40	0.43	4.1	0.20	4.14	13.74
Dub-03	23.5	13.1	22.2	20	4	56	20	365	0.14	0.31	0.45	3.8	0.35	2.91	8.66
Upper oil shale layer															
Dub-05	28.0	19.8	29.7	8	1	44	46	207	0.07	0.23	0.62	5.9	0.39	4.75	8.40
Dub-07	31.0	16.8	26.0	10	2	52	36	485	0.07	0.31	0.53	4.2	0.31	4.74	10.32
Dub-09	34.0	11.0	25.1	19	5	62	13	655	0.09	0.42	0.40	4.4	0.20	5.25	19.64
Dub-12	38.5	41.9	48.4	5	2	61	32	392	0.04	0.28	0.62	6.4	0.39	8.77	19.46
Dub-14	41.5	28.2	17.7	9	4	51	36	271	0.04	0.23	0.65	5.5	0.36	8.32	17.76
Dub-17	46.0	28.3	21.8	15	4	53	28	1005	0.03	0.24	0.68	10.3	0.37	17.19	32.09
Dub-20	50.5	27.3	35.6	9	3	42	46	419	0.05	0.26	0.62	6.4	0.32	3.75	10.42
Dub-21	52.0	11.8	27.5	19	3	49	29	921	0.06	0.28	0.59	5.9	0.32	4.62	13.39
Dub-23	55.0	11.6	36.0	16	3	54	26	535	0.13	0.24	0.54	5.3	0.48	8.52	16.98
Dub-25	58.0	8.8	26.8	18	4	68	10	207	0.17	0.28	0.43	3.3	0.30	2.03	4.15
Dub-27	60.0	8.5	32.1	15	3	66	16	188	0.18	0.24	0.49	3.8	0.36	2.31	4.55
Dub-30	64.5	3.2	68.7	22	5	67	7	1795	0.15	0.54	0.21	3.4	0.12	1.24	7.58
Dub-33	69.0	13.4	26.2	18	11	41	29	550	0.08	0.31	0.51	4.6	0.13	3.87	20.22
Dub-35	72.0	8.5	48.9	15	4	60	21	2261	0.07	0.44	0.42	4.9	0.13	1.92	9.23
Dub-38	76.5	19.1	26.5	15	5	55	24	424	0.06	0.33	0.53	4.8	0.13	4.48	25.64
Dub-40	79.0	7.0	37.7	20	4	69	6	641	0.15	0.39	0.35	3.2	0.23	2.99	10.85
Dub-42	81.0	12.4	42.1	8	3	80	9	51	0.34	0.29	0.27	2.6	0.42	1.09	1.98
Dub-45	86.0	25.3	11.5	10	3	52	35	105	0.10	0.27	0.53	3.8	0.59	5.09	6.76
Main coal seam															
Dub-46	87.5	32.4	19.5	9	5	52	34	62	0.15	0.22	0.49	3.0	0.45	1.42	2.25
Dub-47	89.0	51.6	28.8	6	5	56	32	96	0.10	0.20	0.62	4.6	0.51	9.63	14.94
Dub-48	90.5	63.1	10.1	7	7	56	30	38	0.09	0.23	0.62	5.8	1.57	6.36	3.13
Lower oil shale layer															
Dub-59	152.0	27.3	26.5	9	2	41	47	607	0.09	0.29	0.53	4.5	0.49	2.73	6.82
Dub-64	159.5	9.3	24.1	22	2	51	25	3001	0.06	0.28	0.58	5.5	0.65	4.07	5.77
Dub-74	174.5	21.4	22.5	12	5	62	21	261	0.16	0.24	0.51	4.6	0.92	1.60	1.84
Coal lense															
Dub-77	194.0	46.5	3.9	14	5	59	22	47	0.14	0.17	0.62	5.4	0.96	1.81	1.74

Bulk organic geochemical parameters, conentration and contentration ratios of specific biomarker (TOC: total organic carbon; EOM: extractable organic matter;
Sat. HC: saturated hydrocarbon; Aro. HC: aromatic hydrocarbons; NSO: heterocompounds; Asphalt.: asphaltenes; CPI: carbon preference index; Pr/Ph: pristane/phytane ratio)

Table 4.3 continued

Sample	Depth (m)	C_{27} Steranes (µg/gTOC)	C_{28} Steranes (µg/gTOC)	C_{29} Steranes (µg/gTOC)	Steranes (µg/gTOC)	Hopanes (µg/gTOC)	GI	Steroids (µg/gTOC)	Hopanoids (µg/gTOC)	Steroids/ Hopanoids	Diterpenoids (µg/gTOC)	Triterpenoids (µg/gTOC)	Di-/(Di + Tri)-terpenoids	Arb.(Fern.)-deriv. (µg/gTOC)	Carotenoide (µg/gTOC)
Bituminous marlstone															
Dub-01	13.0	42	140	207	390	177	0.11	419	195	2.14	150	6	0.96	7	161
Dub-02	17.0	48	180	282	511	231	0.14	583	272	2.14	24	18	0.58	31	130
Dub-03	23.5	27	25	38	91	162	0.28	104	213	0.49	27	70	0.28	40	16
Upper oil shale layer															
Dub-05	28.0	18	10	21	50	103	0.16	55	130	0.42	102	22	0.82	25	23
Dub-07	31.0	26	28	41	94	187	0.18	105	243	0.43	9	44	0.17	34	20
Dub-09	34.0	37	93	118	247	263	0.40	325	364	0.89	15	23	0.39	15	163
Dub-12	38.5	12	7	9	29	119	0.19	36	201	0.18	10	50	0.16	113	12
Dub-14	41.5	15	15	20	51	191	0.28	59	319	0.19	4	171	0.02	149	13
Dub-17	46.0	32	13	50	95	357	0.16	104	537	0.19	9	127	0.07	22	39
Dub-20	50.5	16	17	33	66	126	0.21	71	177	0.40	9	36	0.20	36	48
Dub-21	52.0	15	23	30	69	114	0.12	79	154	0.52	11	18	0.38	8	35
Dub-23	55.0	36	13	48	97	220	0.15	104	315	0.33	18	58	0.24	15	47
Dub-25	58.0	71	53	126	249	412	0.20	260	566	0.46	8	67	0.11	22	96
Dub-27	60.0	37	19	64	119	205	0.32	125	268	0.47	25	48	0.35	20	72
Dub-30	64.5	80	61	182	323	455	0.39	323	500	0.65	22	15	0.60	3	325
Dub-33	69.0	20	25	37	82	147	0.10	88	169	0.52	6	11	0.36	3	53
Dub-35	72.0	90	95	200	385	566	0.28	401	656	0.61	10	30	0.26	27	281
Dub-38	76.5	15	38	56	110	153	0.18	114	190	0.60	8	13	0.38	6	81
Dub-40	79.0	49	44	93	186	377	0.15	186	447	0.41	18	38	0.32	51	106
Dub-42	81.0	12	9	40	60	140	0.12	63	193	0.33	7	64	0.09	44	110
Dub-45	86.0	11	5	14	31	78	0.07	33	114	0.29	3	13	0.16	3	6
Main coal seam															
Dub-46	87.5	24	10	21	56	227	n.d.	63	385	0.16	6	194	0.03	135	6
Dub-47	89.0	10	7	15	32	67	n.d.	38	130	0.30	11	162	0.06	135	7
Dub-48	90.5	n.d.	n.d.	n.d.	n.d.	16	n.d.	3	24	0.12	17	71	0.19	13	0
Lower oil shale layer															
Dub-59	152.0	19	22	31	72	199	n.d.	89	274	0.32	8	52	0.13	9	6
Dub-64	159.5	22	26	37	86	360	0.09	86	402	0.21	35	25	0.59	17	9
Dub-74	174.5	14	13	30	57	263	0.25	96	391	0.25	9	144	0.06	57	11
Coal lense															
Dub-77	194.0	1	1	2	4	21	n.d.	12	29	0.40	2	39	0.05	5	0

Conentration and contentration ratios of specific biomarker (Arb.(Fern.)-deriv.: arborene or fernene derivates); n.d.: not defined

The extractable organic matter (EOM) yields vary between 3 and 69 mg/g TOC (average 29 mg/g TOC). The extracts from most samples are dominated by NSO compounds (41-80% of EOM) and asphaltenes (6-47% of EOM). The proportion of hydrocarbons is low. Saturated hydrocarbons are predominant over aromatic hydrocarbons and the relative percentages of both together vary between 7 and 33% of the EOM, as typical for sediments and coals of low maturity (Tissot and Welte, 1984)

Total ion chromatogram traces (TICs) of alkane fractions of representative samples from the bituminous marlstone layer, the upper oil shale layer and the main coal seam are shown in Figure 4.8. Traces based on a mass range of 191 (Hopane) and 217 (Sterane) of the same samples are presented in Figure 4.11. A gas chromatogram of aromatic hydrocarbon fractions of a representative sample in the upper oil shale layer is shown in Figure 4.12.

Straight chain alkanes, isoprenoids

The saturated hydrocarbon fractions of most samples are dominated by *n*-alkanes from *n*-C_{15} to *n*-C_{32}. Highest relative abundances are seen in intermediate chain *n*-alkanes (*n*-C_{21-25}) ranging from 17 to 54% and long chain *n*-alkanes (*n*-C_{27-31}) ranging from 21 to 68% (Table 4.3). The relative distribution of short-, intermediate-, and long chained *n*-alkanes are shown in Figure 4.6. While long chain *n*-alkanes are known as biomarkers for higher terrestrial plants, as they are the main components of plant waxes (Eglinton and Hamilton, 1967), *n*-alkanes of intermediate molecular weight originate according to Ficken et al. (2000) from aquatic macrophytes. Members of low molecular weight (*n*-C_{15-19}) are present in relative abundances from 3 to 18% of total *n*-alkanes and are found in algae and microorganisms (Cranwell, 1977). An exception shows Dub-42 (81 m), where *n*-alkanes of short chain length are predominant with 34% over intermediate and long chain homologous.

The distributions of *n*-alkanes with a marked odd over even predominance display maxima at *n*-C_{27}. It was considered as a reliable proof that the organic matter originates from higher terrestrial plants (Tissot and Welte, 1984). However, the same distribution has been found in sediments which originate from the freshwater alga Botryococcus (Lichtfouse et al., 1994; McKirdy et al., 1986). The distribution of *n*-alkanes with the domination of odd members and with maxima at *n*-C_{23} indicates the low degree of maturity and algal origin of the organic substance (Hunt et al., 1979; Volkman et al., 1986). In most analysed samples intermediate and long chained *n*-alkanes are dominated by odd numbers with maxima at *n*-C_{27}. Both samples, Dub-02 and Dub-30, are also characterized by a domination of odd members however the maxima is at *n*-C_{23}. In short chained *n*-alkanes odd- and even-carbon numbers show a similar distribution. On basis of the distribution of *n*-alkanes the carbon preference index (CPI) varies between 2.6 and 6.4 with an exception of 10.3 in Dub-17.

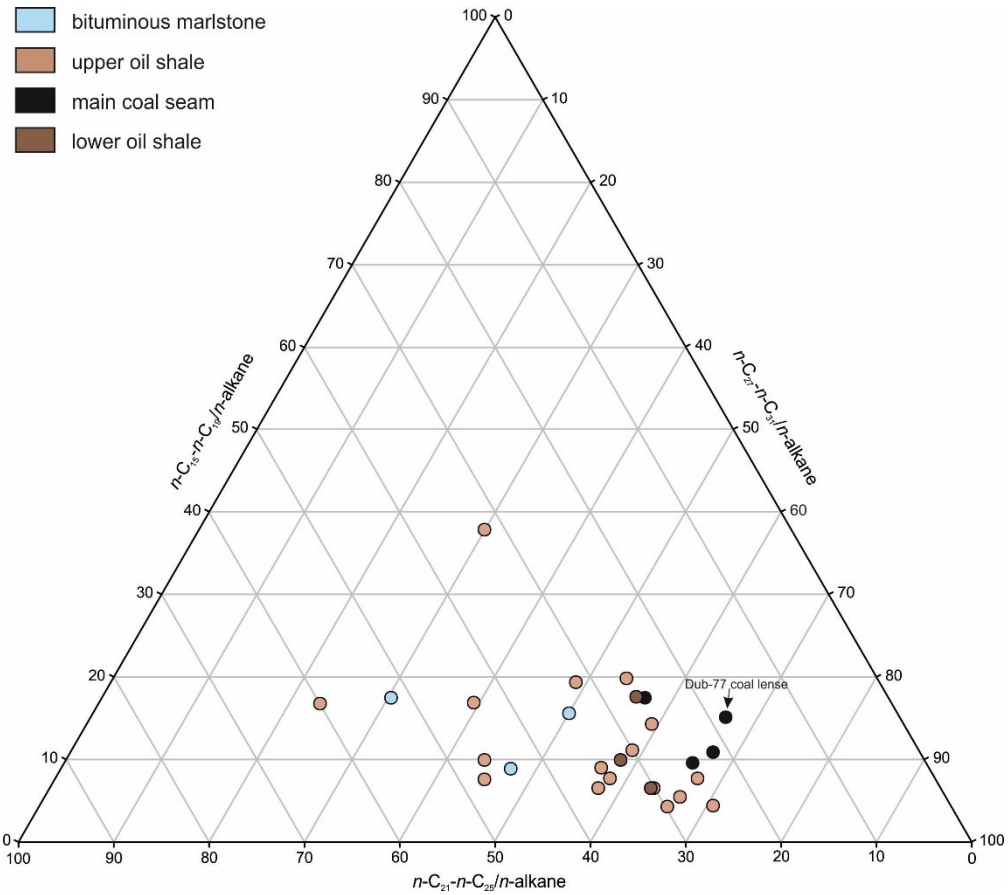

Figure 4.6: Relative distribution of short (n-C_{15-19}), intermediate (n-C_{21-25}) and long chained (n-C_{27-31}) n-alkanes

The acyclic isoprenoids pristane and phytane are found in all analysed samples. According to Didyk et al. (1978) the most abundant source of pristane (C_{19}) is the phytyl side chain mainly derived from chlorophyll "a" molecule in phototrophic organisms. Under oxic conditions the phytyl side chain is formed to phytol. Then phytol is converted to phytenic acid before decarboxylation to pristene, and hydrogenation to pristane. According to the same authors the most abundant source of phytane (C_{20}) is the phytyl side chain also mainly derived from chlorophyll "a" molecule in phototrophic organisms, although it has been found in methanogenic bacteria. In reducing environments phytane is formed by hydrogenation of phytol to dihoydrophytol and then to phytane.

The Pr/Ph ratio (Figure 4.9a) can give an insight into the conditions of source rock deposition and is regarded as redox parameter. A reducing deposition environment is characterised by a higher abundance of phytane and in consequence by a ratio below 1.0. According to Didyk et al. (1978), Pr/Ph ratios below 1.0 indicate anoxic conditions during early diagenesis. Values between 1.0 and 3.0 were interpreted as indicating dysoxic environments. All samples above the main coal seam show Pr/Ph ratios between 0.1 and 0.5. Approaching the main coal seam, ratios rise up to a maximum of 1.6 in Dub-48. Samples below the main coal seam show by trend higher ratios than samples above.

The ratio between the acyclic isoprenoids and *n*-alkanes can be used to estimate the origin of the organic matter and its maturity (Pr/*n*-C_{17} and Ph/*n*-C_{18}). Lower plants, algae and bacteria contain smaller quantities of *n*-alkanes relative to acyclic isoprenoids, compared to the higher terrestrial plants (Tissot and Welte, 1984). Relative to *n*-alkanes, pristane and phytane is dominating in all analysed samples (Table 4.3). A cross-correlation of Pr/*n*-C_{17} versus Ph/*n*-C_{18} is shown in Figure 4.7. The ratios increase significantly with biodegradation and decrease with thermal maturity. All analysed samples indicate an immature stage and support deposition under reducing (anoxic) environment. Only coal sample Dub-48 was formed under oxic conditions.

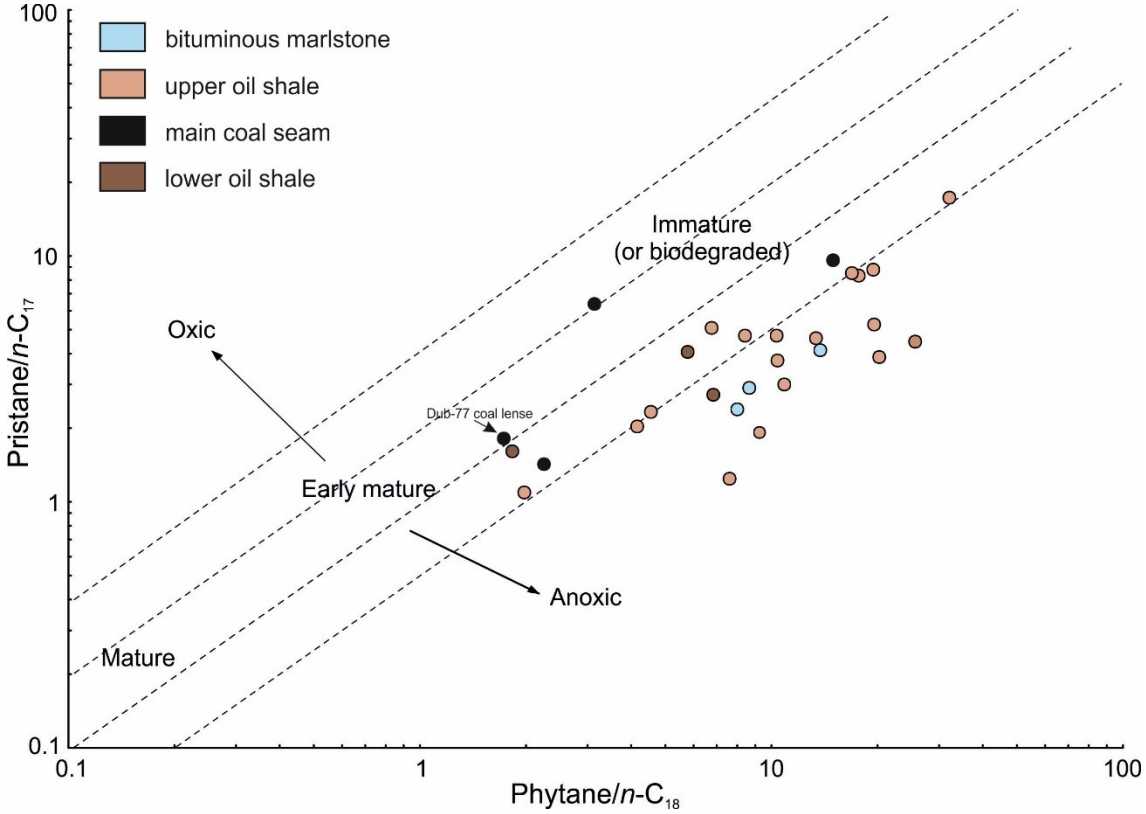

Figure 4.7: Cross-correlation of pristane/n-C_{17} versus phytane/n-C_{18} ratios (according to Connan and Cassou, 1980)

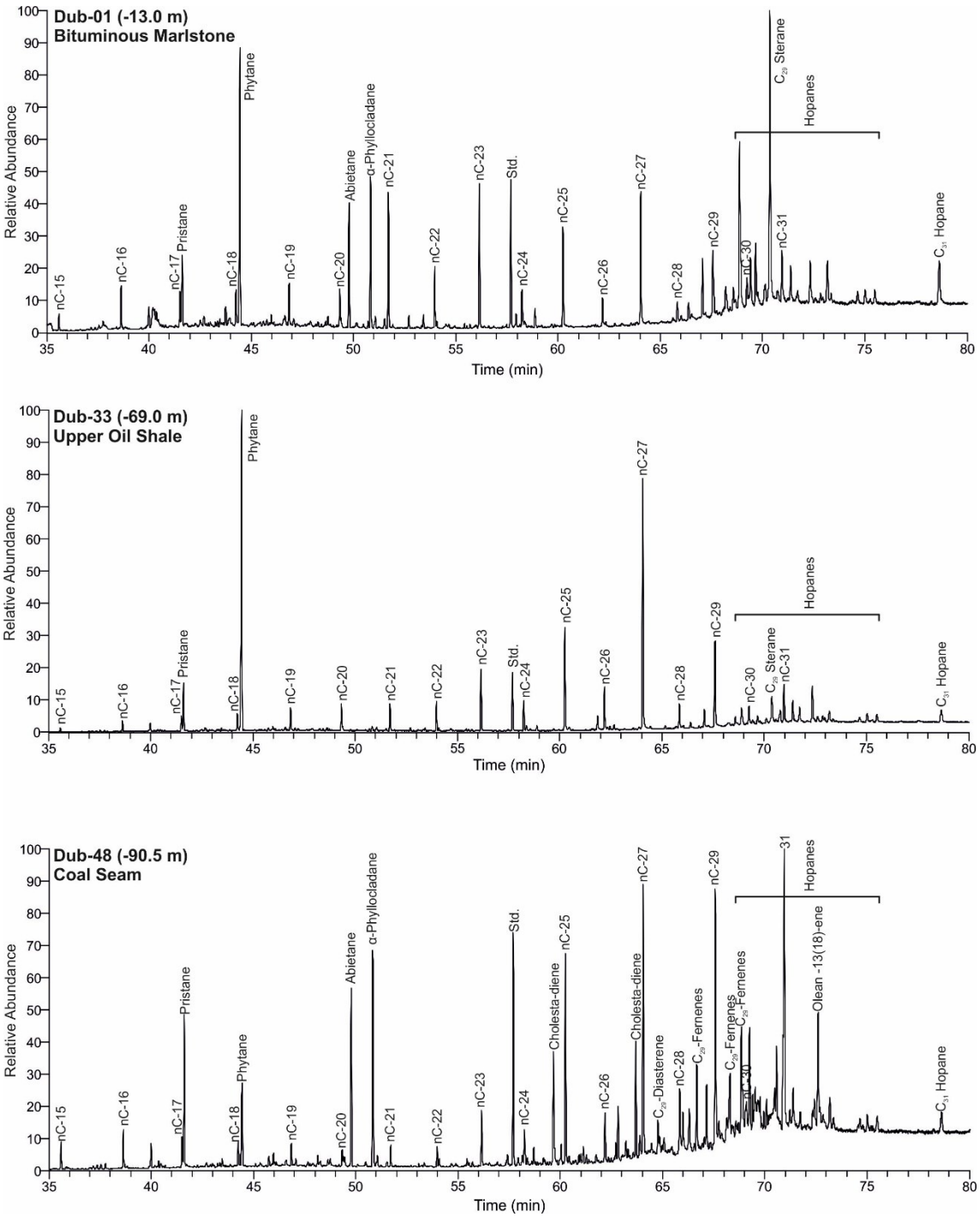

Figure 4.8: Gas chromatograms (TICs) of saturated hydrocarbon fractions of samples from the Aleksinac coal seam, the upper oil shale and the bituminous marlstone. n-alkanes are labelled according to their carbon number. Std: standard (1,1-binaphtyl)

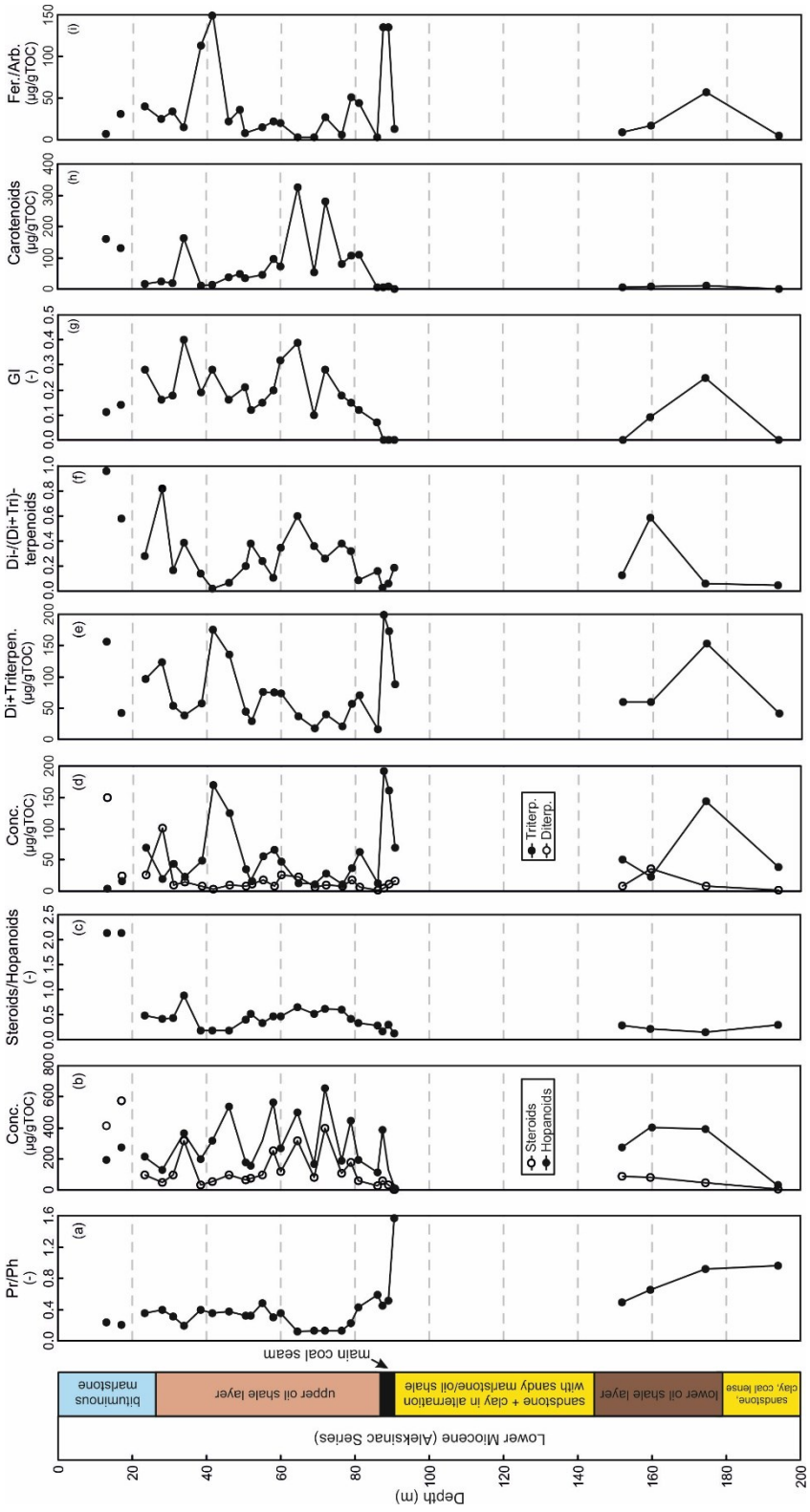

Figure 4.9: Distribution of (a) pristane/phytane ratio, (b) steroid and hopanoid concentrations, (c) steroids/hopanoids ratio, (d) diterpenoid and non-hopanoid triterpenoid concentrations, (e) sum of diterpenoid and non-hopanoid triterpenoid concentrations, (f) ratio of diterpenoids to the sum of diterpenoids plus non-hopanoid triterpenoids, (g) Gammacerane index (GI), (h) carotenoids concentrations, (i) sum of fernene and arborene derivates concentrations

Steroids, Hopanoids

In the saturated hydrocarbon fractions C_{27}, C_{28} and C_{29} steranes were detected. The relative percentages and the origin of the organic matter are shown in Figure 4.10. In the bituminous marlstones and the upper oil shale layer mostly C_{29} steranes predominate with around 50%, followed without distinct trend by C_{28} or C_{27} steranes. Corresponding diasterenes were only found in low quantities of C_{29}. In the coal sample Dub-48 steranes cannot be quantified. Only C_{29} diasterene and cholestadien as a precursor of C_{27} sterane are present. Below the coal seam again C_{29} steranes predominate with around 45% followed by C_{28} and the C_{27} steranes. While algae are the biological source of C_{27} sterols, the predominant primary producers of C_{29} sterols are photosynthetic organisms, including landplants (Volkman, 1986). Also special freshwater green algae like ulvophytes and early diverging prasinophyte produce high abundances of C_{29} sterols. Other plausible candidates include the glaucocystophytes and early divergent red algae (Kodner et al., 2008). Also cyanobacteria can produce C_{29}-sterols (Huang and Meinschein, 1979). The TOC-normalized amounts of the sum of identified steroid compounds (steranes plus C_{29} diasterene) are given in Table 4.3. Concentrations of steroids vary in the bituminous marlstones from 104 to 583 µg/g TOC and in the upper oil shale layer between 36 and 402 µg/g TOC. In the coal seam steroid concentration goes down to 3 µg/g TOC and in samples below the main coal seam concentration varies within comparable ranges between 85 and 95 µg/g TOC. No depth trend of steroid concentrations exists within the profile (Figure 4.9b).

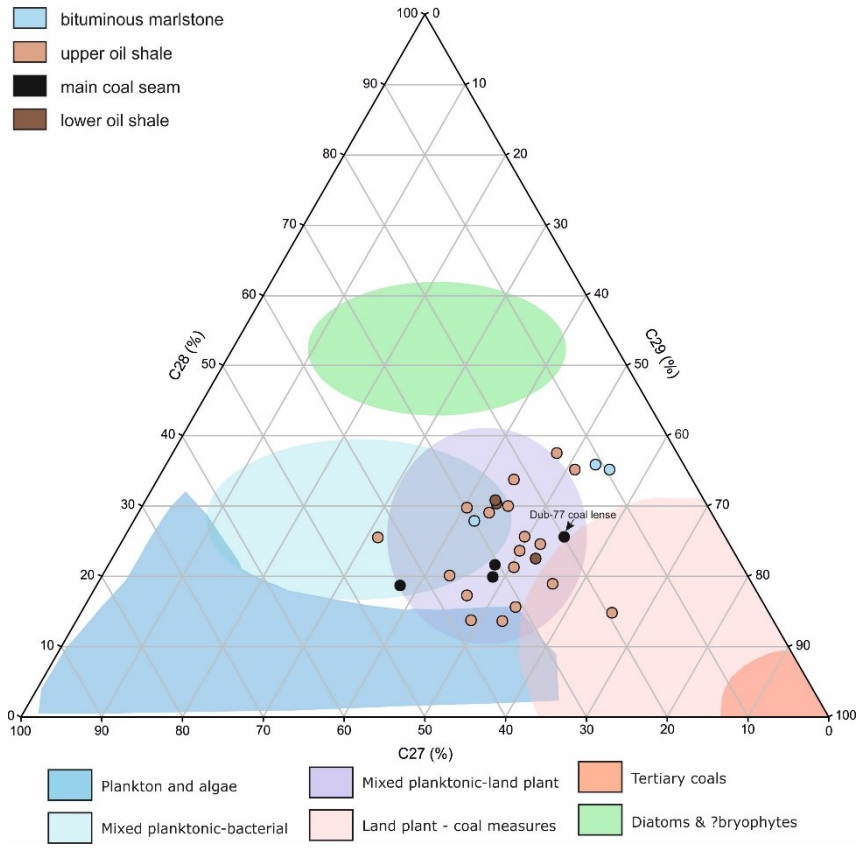

Figure 4.10: Ternary diagram of C_{27}, C_{28} and C_{29} steranes (after Hunt, 1996)

Hopanes are important constituents of the non-aromatic cyclic triterpenoids concentrations. The hopanoid patterns are characterized by the occurrence of αβ-type and βα-type hopanes from C_{27} to C_{31}, the C_{28} hopanes are absent. The predominant hopanoid in samples of the upper oil shale layer above 55 m is the hop-17(21)-ene. Below this depth 17α,21β-C_{30}-hopane dominates till the main coal seam where 17β,21α-C_{30}-hopane prevails. C_{30} Hop-13(18)-ene occurs in low intensities within the GC traces of the upper oil shale layer. In Dub-48 (main coal seam) C_{27}-, C_{28}-, C_{29}- and C_{30} Hop-13(18)-enes are present. In samples below the coal seam C_{30} Hop-13(18)-ene occurs in high intensities. The biological source of hop-17(21)-ene has not been clarified so far, most likely anaerobic, iron reducing bacteria are suggested (Bechtel et al., 2002). According to Volkman et al. (1986) and Wakeham (1990), the compound is directly contributed to the sediment by bacteria. Apart from a direct input, hop-17(21)-ene was proposed to be a diagenetic product of hop-22(29)-ene (Brassell et al., 1980) which in turn might originate from diplopterol found in several eukaryotic phyta (e.g. ferns, mosses, lichens, fungi) as well as in iron reducing anaerobic bacteria (Bottari et al., 1972; Ourisson et al., 1979; Rohmer and Bisseret, 1994; Wolff et al. 1992).

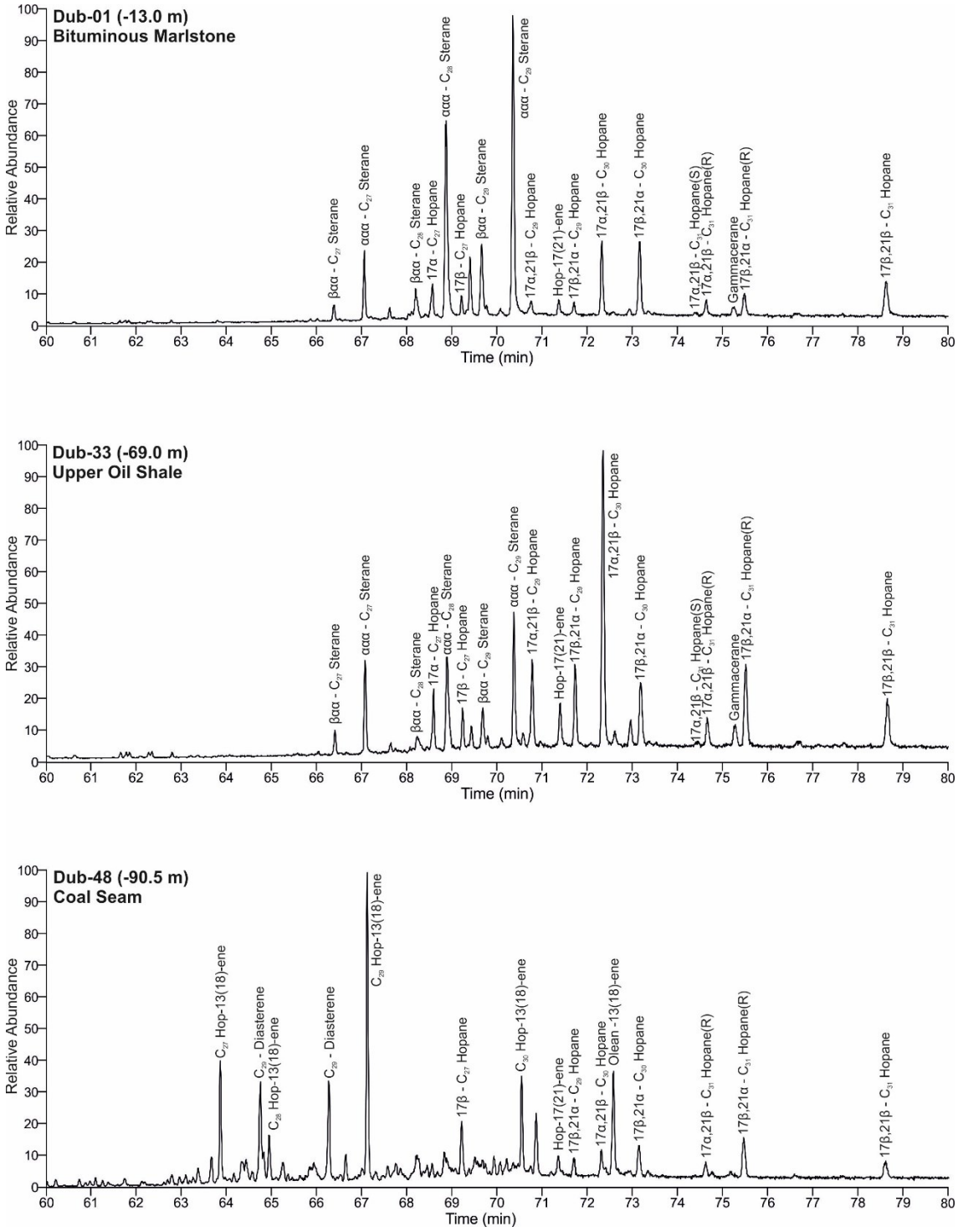

Figure 4.11: Gas chromatograms (mass range 191 (hopanes) and 217 (steranes)) of saturated hydrocarbon fractions of samples from the Aleksinac coal seam, the upper oil shale and the bituminous marlstone

Gammacerane is present with moderate concentrations in all layers except in the main coal seam. It is a marker for a stratified water column during source-rock deposition, commonly associated with elevated salinity, as in alkaline lakes and lagoonal carbonate evaporites (Sinninghe Damste et al., 1995). The Gammacerane index (GI) was calculated through the ratio of gammacerane to C_{30} hopane and varies in the upper oil shale layer between 0.07 and 0.40 and is not present in the main coal seam (Figure 4.9g). A series of C_{32}- to C_{34}-benzohopanes is identified in relative low concentrations in the aromatic hydrocarbon fractions. Oils and bitumen from evaporitic and carbonate source rocks show the highest concentrations of benzohopanes (e.g. He W. and Lu S., 1990). Generally hopanoids show an input from bacterial biomass (Ourisson et al., 1979, Rohmer et al., 1984). Their concentrations vary in the upper and the lower oil shale layer between 113 and 656 µg/g TOC. In the main coal seam (Dub-48) and in the coal sample Dub-77 concentrations are with around 25 µg/g TOC clearly lower (Table 4.3).

The vertical variation of steroids and hopanoids is visible in Figure 4.9b where the relative increase and decrease of both biomarker groups correlate very well with each other. In Figure 4.9c the steroids to hopanoids ratio is presented. Except of the uppermost two samples in the bituminous marlstone layer the ratios are below 1.0.

Diterpenoids, non-hopanoid triterpenoids

Constituents of the saturated diterpenoids originate mainly from gymnosperms (conifers) and include norpimarane, pimarane, abietane and α-phyllocladane, (Hagemann and Hollerbach, 1979; Noble et al., 1985; Philp, 1985). α-Phyllocladane predominates by far in all samples (Figure 4.8). The corresponding aromatic diterpenoids occur in the gas chromatograms of the aromatic hydrocarbon fractions (Figure 4.12) and consist of compounds of the abietane type (e.g. abieta-tetraene, norabietatriene, simonellite and retene; Philp, 1985).

In addition saturated non-hopanoid triterpenoids have been identified as biomarkers for angiosperms (flowering landplants). They contain especially the structures of des-A-oleanenes, olean-13(18)-ene, des-A-ursane and des-A-lupane, which indicate low maturity. Aromatic non-hopanoid triterpenoids include mainly olean-12-ene and dimethyltetrahydropicene and in minor abundances triaromatics and tetraaromatics (ten Haven et al., 1992; Logan and Eglinton, 1994; Philp, 1985; Rullkötter et al., 1994). Angiosperm biomarkers represent an input of leafs, waxes, wood, roots or bark (Karrer et al., 1977).

In Figure 4.9d the concentration variations of diterpenoids (average 22 µg/g TOC) and non-hopanoid triterpenoids (average 63 mg/g TOC) are indicated. Figure 4.9e shows the sum of them with a maximum in Dub-46 (200 µg/g TOC). The ratio of gymnosperms to the sum of gymnosperms plus angiosperms (di-/di-+triterpenoids) is selected as the best quantitative expression of landplant derived biomarker contribution (Figure 4.9f). The data indicate the predominance of angiosperms in most analysed samples.

Further identified biomarkers

Tricyclic terpanes were identified in all samples in relative low concentrations (< 7 µg/g TOC). They could originate from terrigenous plants in addition to bacterial or algal sources and indicate sedimentation in freshwater lakes or saline environment. If the concentration is low, tricyclic terpanes are linked as biomarkers in freshwater source rocks (Peters, 2000).

Carotenoids comprise a wide range of C_{40} compounds produced mainly by photosynthetic organisms (algae). Because carotenoids are easily oxidized, they are rarely found in sediments (Repeta and Gagosian, 1987; Repeta, 1989). Under highly reducing conditions, the carotenoid skeleton may be preserved in sediments. A geochemically important carotenoid is β-carotane, which develops through the reduction of β-carotene in low-sulphur anoxic lacustrine systems. The presence of relatively high concentrations of β-carotane, suggests source input dominated by species of halophilic bacteria (Jiang and Fowler, 1986) or cyanobacteria (Brocks et al., 2005). Concentrations of β-carotane vary in a wide range between 4 and 295 µg/g TOC in the oil shale layers and are absent in coal samples. Gamma(γ)-carotane commonly occurs with β-carotane. The ratio of γ- to β-carotane increases with thermal maturity and decreases with biodegradation, but the ratio is also affected by source organic matter input (Jiang and Fowler, 1986). In all analysed samples γ-carotane does not exist. In aromatic hydrocarbons carotenoids occur in the oil shales in form of a C_{40} monoaromatic carotenoid in concentrations between 1 and 83 µg/g TOC. Again this carotenoid was not detected in coal samples. In Dub-42 occurs β-Renierapurpurane, which is recorded as carotenoid derivate and can be derived from purple sulphur bacteria or green sulphur bacteria (Brocks and Schaeffer, 2008). The sum of saturated and aromatic carotenoids is shown in Figure 4.9h.

Fernenes and their aromatic derivates are biomarkers of ferns and indicators for floral input, specific to pteridosperms (seed ferns) and coniferophytes (dominant landplants) (Paull et al., 1998). Volkman et al. (1986) however, correlated fernene with high concentrations of methanogenic biomarkers and suggested that it might originate from purple sulphur bacteria as a marker for anoxic depositional environment. Fernenes (C_{29} fernenes) in the saturated hydrocarbons are only identified in low amounts (<10 µg/g TOC) in the main coal seam. Onocerane, a biomarker originating from ferns, is present in Dub-48. A mixture of aromatic fernene derivates and arborene derivates occur in all analysed samples of the aromatic hydrocarbon fraction. Their concentrations vary between 1 and 148 µg/g TOC and are shown in Figure 4.9i. It is difficult to distinguish between aromatized derivates of fernene and arborene, because the carbon skeletons of their series are identical (except the orientation around the optical centres).

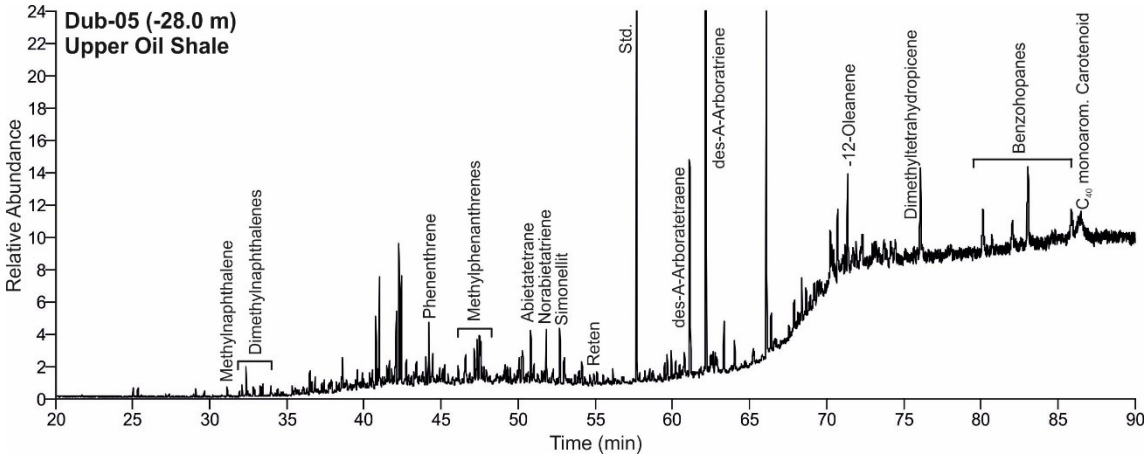

Figure 4.12: Gas chromatogram (TIC) of the aromatic hydrocarbon fraction of sample Dub-05 from the upper oil shale layer. Std: standard (1,1-binaphtyl)

4.4 Stable isotope geochemistry

The organic carbon isotope ratios are listed in Table 4.4.

Table 4.4: Organic carbon isotope ratios

Sample	Depth (m)	$\delta^{13}C$ (‰)
Bituminous marlstone		
Dub-01	13,00	-30,38
Dub-02	17,00	-30,24
Dub-03	23,50	-29,29
Upper oil shale layer		
Dub-04	26,50	-27,98
Dub-05	28,00	-29,15
Dub-06	29,50	-30,08
Dub-07	31,00	-30,46
Dub-08	32,50	-29,68
Dub-09	34,00	-31,07
Dub-10	35,50	-29,79
Dub-11	37,00	-28,86
Dub-12	38,50	-26,92
Dub-13	40,00	-30,17
Dub-14	41,50	-30,17
Dub-15	43,00	-30,33
Dub-16	44,50	-29,00
Dub-17	46,00	-29,49
Dub-18	47,50	-29,32
Dub-19	49,00	-31,15
Dub-20	50,50	-31,17
Dub-21	52,00	-31,01
Dub-22	53,50	-29,75
Dub-23	55,00	-30,30
Dub-24	56,50	-30,81
Dub-25	58,00	-31,28
Dub-26	58,50	-31,39
Dub-27	60,00	-30,50
Dub-28	61,50	-30,40
Dub-29	63,00	-32,05
Dub-30	64,50	-28,15
Dub-31	66,00	n.d.
Dub-32	67,50	-30,09
Dub-33	69,00	-30,46
Dub-34	70,50	-30,57
Dub-35	72,00	-29,62
Dub-36	73,50	n.d.
Dub-37	75,00	-31,05
Dub-38	76,50	-30,89
Dub-39	78,00	-29,16
Dub-40	79,00	-29,84
Dub-41	80,00	n.d.
Dub-42	81,00	-30,52
Dub-43	83,00	-30,64
Dub-44	84,50	-30,08
Dub-45	86,00	-28,71
Main coal seam		
Dub-46	87,50	-28,12
Dub-47	89,00	-26,09
Dub-48	90,50	-25,93
Sandstone and clay		
Dub-49	95,00	n.d.
Dub-50	130,00	-26,74
Dub-51	140,00	-25,82
Dub-52	141,50	-26,47
Dub-53	143,00	-25,77
Dub-54	144,50	-26,04
Lower oil shale layer		
Dub-55	146,00	-28,25
Dub-56	147,50	-26,32
Dub-58	150,50	-29,22
Dub-59	152,00	-27,80
Dub-60	153,50	-30,25
Dub-61	155,00	-28,25
Dub-62	156,50	-30,49
Dub-63	158,00	-29,97
Dub-64	159,50	-30,36
Dub-65	161,00	-25,67
Dub-66	162,50	-27,87
Dub-67	164,00	-24,72
Dub-68	165,50	-27,59
Dub-69	167,00	-27,63
Dub-70	168,50	-27,57
Dub-71	170,00	-27,53
Dub-72	171,50	-27,04
Dub-73	173,00	-25,88
Dub-74	174,50	-28,69
Dub-75	176,00	-29,42
Sandstone interbedded with oil shale and coal lenses		
Dub-76	192,50	-28,11
Dub-77	194,00	-25,51
Dub-78	195,50	-25,67
Dub-79	197,00	-24,98
Dub-80	198,50	-26,74
Dub-81	200,00	-24,63
Dub-82	201,50	-26,86
Dub-83	203,00	-25,47
Dub-84	204,50	n.d.
Dub-85	206,00	n.d.
Dub-86	208,50	-26,40
Dub-87	210,00	-27,63
Dub-89	213,00	-24,71

n.d.: not defined

Stable isotopes are used to characterize organic matter in source rocks, with emphasis on stable carbon isotope ratios. Stable isotope ratios are reported in delta notation ($\delta^{13}C$, Coplen, 2011) relative to the V-PDB standard. Organisms generally prefer ^{12}C over ^{13}C, which leads to an enrichment of ^{12}C over ^{13}C in most types of organic matter (Naafs, 2016). Figure 4.1g shows the vertical variation of $\delta^{13}C$ of total organic matter. Samples from coaly layers and the main coal seam have typically heavier $\delta^{13}C$ values (^{13}C enriched; $\delta^{13}C$ = -28 to -26‰) than samples taken from the bituminous marlstones and oil shales (^{13}C depleted; $\delta^{13}C$ = -31 to -29‰). This is referable to heavier $\delta^{13}C$ values in terrigenous organic matter and lighter $\delta^{13}C$ values in algal organic matter. The coal samples Dub-48, Dub-47 and Dub-46 show ^{13}C enrichment due to terrigenous organic matter input and oxic environment. A positive correlation between HI and $\delta^{13}C$ (r^2=0.57) indicates that a high HI is associated with lighter $\delta^{13}C$ values. Samples with high contents of hopanoids and low concentration of steroids are characterized by more negative $\delta^{13}C$ values. In sample Dub-30 at around 65 m depth, vitrinite and liptinite of terrigenous origin are increased (Figure 4.1h), also indicated through a heavier value of $\delta^{13}C$ in Figure 4.1g and a lower HI in Figure 4.1c. In lacustrine sediments $\delta^{13}C$ is often not very diagnostic because it is a mixture of many different types of organic matter (algae and terrigenous liptinite, vitrinite and inertinite).

5. Discussion

5.1 Maturity

Average vitrinite reflectance of coal (0.54%Rr) and the upper oil shale layer (0.44%R_r) indicate that the organic matter is thermally immature (to marginally mature). This interpretation is supported by low production index values (PI: ~0.01). T_{max} values of type I kerogen is a poor maturity parameter, but low T_{max} values of samples with type III kerogen (410-440°C) are additional proof for the low maturity of the studied succession.

5.2 Depositional environment

In the following sections bulk parameter, organic petrography and biomarker proxies are used to reconstruct the depositional environment of the main coal seam, the upper oil shale layer and the bituminous marlstone layer. Based on these data the deposition of these layers was subdivided into five stages as illustrated in Figure 5.1.

Due to less information about the layers below the main coal seam, the depositional environment of these samples is not discussed here in detail. Note that sample Dub-77 has similarities with the coal sample Dub-48. The samples Dub-74, Dub-64 and Dub-59 are in a similar range of those from the upper oil shale layer.

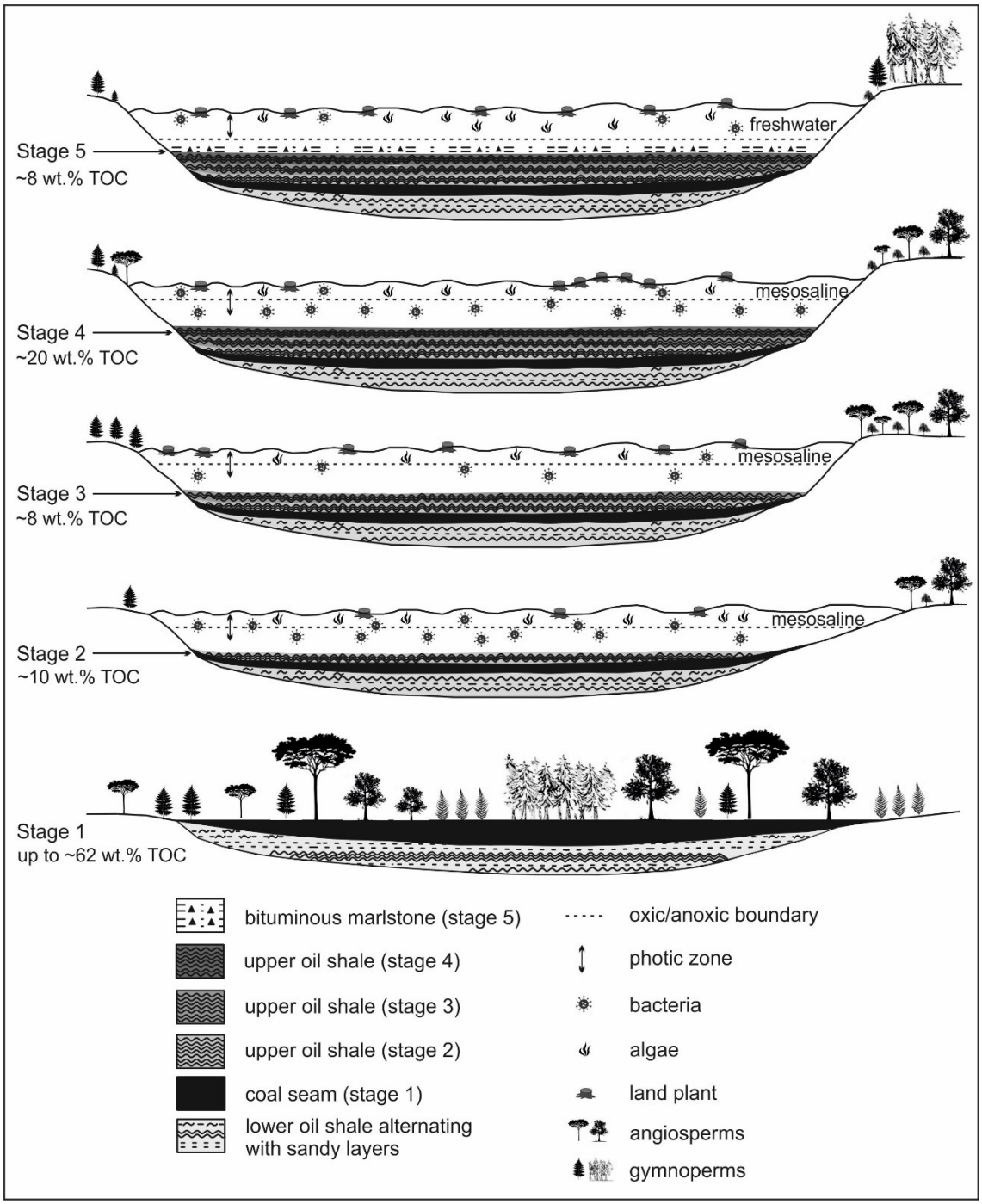

Figure 5.1: Cartoon illustrating the depositional environment of the main coal seam and the overlying upper oil shale and bituminous marlstone

Main coal seam (stage 1; Dub-48 to 46)

The main coal seam in borehole BD-4/2011 is represented by samples Dub-48 to Dub-46. These samples show a trend from a shaly coal with high TOC and low mineral matter content (Dub-48) to a coaly shale (Dub-46). The presence of alginite and moderately high to high mineral matter contents reflects subaquatic deposition in a drowning low-lying mire. High percentages of vitrinite (>80 vol.%) and moderate percentages of inertinite macerals (1-5 vol.%) reflect the input of higher landplants, which according to biomarker analysis was dominated by angiosperms. Onocerane, a biomarker associated with rapid deposition in restricted basins with abundant terrigenous input (Tsuda, 1980), is present. A heavy $\delta^{13}C$ value of -26‰ reflects the enhanced terrestrial input.

Despite high vitrinite percentages, only Dub-48 shows a HI of 112 mgHC/gTOC, whereas the two upper samples are characterized by high HI values (>500 mgHC/gTOC) supporting the presence of hydrogen-rich vitrinite. Hydrogen-rich vitrinite may originate from drift wood that is reworked by bacteria into biomass with higher HI than the original material. Moreover an enhanced content of bituminous matter may be derived from microbial activity during drifting of the wood fragments or after their deposition in the sediment (Schnitzerl and Neuroud, 1975; Mastalerz et al., 1993).

Pr/Ph ratios indicate an oxygenated environment during deposition of Dub-48, whereas the rising water table caused anoxic conditions during deposition of the upper part of the main coal seam (Dub-47, Dub-46). Sulphur contents are high in all samples (3.7-7.5 wt.%). This together with high percentages of framboidal pyrite indicates either a brackish influence or a carbonate-rich environment with relative high pH values (e.g. Diessel, 1992). Because the overlying oil shale is intercalated with dolomite layers (e.g. Kasanin-Grubin, 1997), we prefer the second interpretation.

Upper oil shale layer (stages 2-4; Dub-45 to Dub-05)

At the start of **stage 2** (Dub-45 to Dub-33; 86-69 m) the swamp facies was replaced by a lacustrine environment. TOC contents decrease significantly in the transition zone, but remain in the order of 10 wt.%. Very high percentages of alginite and high HI values (638-886 mgHC/gTOC) indicate the predominance of aquatic organic matter. An additional upward increase in aquatic organic matter during stage 2 is indicated by alginite percentages and HI values.

Steroids are mainly compound by C_{29} steranes, which are rather originate in this case from cyanobacteria or algal lipid sterols and not from higher terrestrial plants. Higher abundances of hopanoids compared to steroids point to the dominant participation of bacterial biomass in sequences of the sediment column. Samples with high contents of hopanoids and low concentration of steroids are characterized by lower $\delta^{13}C$ values. As hopanoids are considered as a measure of microbial activity, this relationship is explained by bacterial carbon shifting of the isotopic

composition of the biomass towards more negative values. Also an enhanced content of algae in the samples lead to ^{13}C depletion.

Low concentrations of landplant-derived biomarkers show that the input of terrestrial plants was minor. Di- and triterpenoids ratios show that the terrestrial organic matter was dominated by angiosperms, although the relative abundance of gymnosperms increases upwards.

The change from the swamp facies to the lacustrine facies was caused by a rise in relative lake level, probably induced by increased subsidence rates. Increasing water depth allowed the establishment of a stratified water column. Upward increasing gammacerane index (GI) values suggest that water column stratification was due to salinity stratification (Sinninghe Damste et al., 1995). An alkaline lake environment is also supported by high sulphur contents, low TOC/S ratios and locally high carbonate contents.

Very low Pr/Ph ratios (<<1) show that water column stratification resulted in strictly anoxic environments. The presence of carotenoids, a biomarker preserved only in reducing conditions, supports this hypothesis. Samples with relative high concentrations of β-carotanoids indicate the presence of halophilic bacteria (Jiang and Fowler, 1986) or cyanobacteria (Brocks et al., 2005). Samples with both, high GI and carotenoid concentrations indicate a mesosalinar environment and strong salinity stratification.

The aquatic organic matter (mainly algae) is isotopically light (-31 to - 29‰). Isotopically light values are interpreted to reflect enhanced accumulation of dissolved CO_2 within the water column, originating from degradation of organic matter by bacterial oxidation (Bechtel and Püttmann, 1997; Hertelendi and Vetö, 1991). In these settings dissolved CO_2 in the photic zone may be composed partly of ^{13}C depleted 'recycled' CO_2 derived from bacterial decomposition. This ^{13}C depleted 'recycled' CO_2 is then absorbed by freshwater algae.

Stage 3 (Dub-32 to Dub-21; 68-51 m): Anoxic, mesosaline-lake environments continued during deposition of the upper oil shale layer. However, an upward decrease in GI suggests that the degree of stratification decreased through time. A parallel decrease in the concentration of carotenoids and a slight increase in Pr/Ph ratios suggests that the weaker water column stratification resulted in a gradual decrease in anoxia.

Relative low TOC contents (3-4 wt.%) and high percentages of terrestrial macerals (>60 vol.%) indicate that accumulation of aquatic organic matter was reduced during the onset of stage 3, which is also reflected by relative low HI values (<600 mgHC/gTOC). Thereafter aquatic bioproductivity recovered. Consequently TOC contents increased to values around 10 wt.% and HI values are in the order of 600 to 800 mgHC/gTOC.

Oil shale with the highest TOC contents (~20 wt.%) have been deposited during **stage 4** (Dub-20 to Dub-04; 51-26 m). A significant increase in TOC/S ratios may indicate a reduction in salinity. However, as sulphur contents remain constant, it is more likely that sulphate availability remained also constant, but that compared to the enormous amount of organic matter, the sulphate reservoir in the pore water was limited. The vertical trend of GI values also does not indicate a significant change in lake water salinity. In contrast, GI data imply that strong salinity stratification persisted during stage 4. Similarly anoxic conditions continued, although reduced concentrations of carotenoids may indicate less reducing conditions.

Organic matter input was dominated by algae and bacteria. Lower plants, algae and bacteria contain smaller quantities of n-alkanes relative to acyclic isoprenoids. This is supported by high Pristane/*n*-C_{17} and Phytane/*n*-C_{18} ratios. Relative high percentages of landplant-derived macerals indicate that a significant amount of terrestrial organic matter was deposited during the middle part of stage 4. High concentrations of non-hopanoid triterpenoids in samples Dub-14 and Dub-17 as well as increased input of oleanene show that the terrestrial organic matter is dominated by angiosperms. Increased input of terrestrial organic matter is also reflected by a zone with reduced HI values.

Organic matter accumulation decreased during the late stages of oil shale accumulation.

Bituminous marlstone (stage 5; Dub-03 to Dub-01)

The lowermost sample (Dub-3) has been deposited in a similar environment than the underlying oil shale.

Low sulphur content, low bacterial sulphate reduction in the bituminous marlstone layer and increasing TOC/S ratios may reflect a trend towards increased fresh water influx and oligotrophic environment. Also a lower GI supports lower salinity. Carotenoids are produced rather by photosynthetic organisms (algae or cyanobacteria) and not by halophilic bacteria. Compared to the other layers it is obvious, that in these samples steroids predominate over hopanoids and diterpenoids over non-hopanoid triterpenoids. Diterpenoids are dominated by abietane and α-Phyllocladane, indicators for resin rich woods. Here the primary production of organic matter is dominated by photosynthetic organisms rather than by bacteria. According to organic petrography, the photosynthetic organisms are predominantly algae and sea plants. $\delta^{13}C$ values of around -31‰ confirm algal domination. Since Pr/Ph ratio is < 1 a reducing deposition environment still prevails.

5.3 Source rock and oil shale potential

Source rock potential

TOC contents and the generative potential (S_1 + S_2) are used to characterize the quality of hydrocarbon source rocks (e.g. Cassa and Peters, 1994). Average TOC (18.0 wt.%) S_1 + S_2 (115 mgHC/g) and HI values (743 mgHC/gTOC) show the excellent source rock quality of the upper oil shale layer. Similar average values are recorded for rocks from the lower oil shale layer (TOC: 20.0 wt.%, S_1 + S_2: 126 mgHC/g; HI: 620 mgHC/gTOC). Both oil shale layers include highly oil-prone type I kerogen.

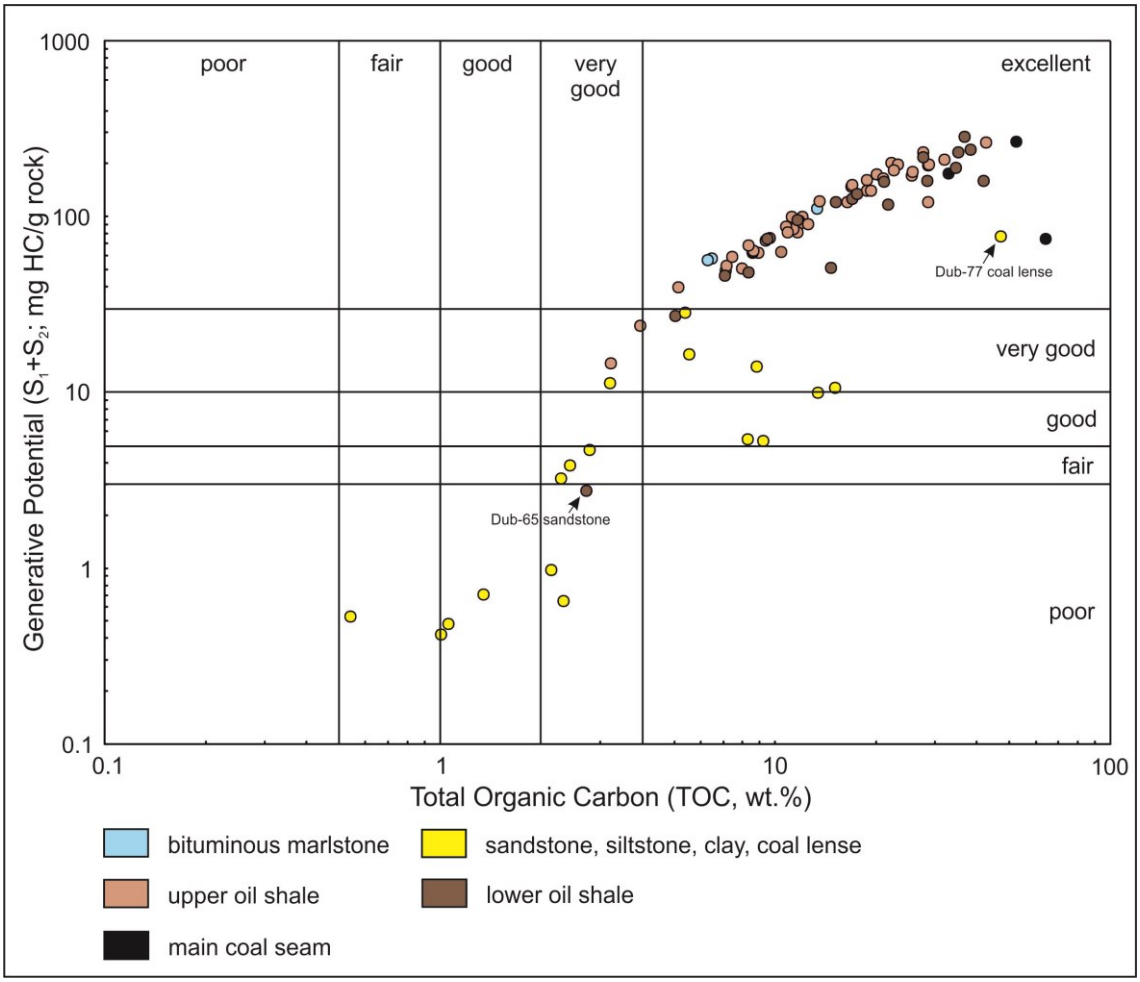

Figure 5.2: Plot of generative potential (S_1 + S_2) versus total organic carbon (TOC) and resulting oil shale potential according to Peters and Cassa (1994)

The excellent source rock quality of the oil shale layers, but also of the main coal seam and samples from the bituminous marlstones, is also obvious from Figure 5.2. In contrast, samples from sandy and clayey layers underlying the main coal seam are poor or fair source rocks. Coaly sediments within these layers are characterized by high TOC contents, but relative low generative potential.

The amount of hydrocarbons, which can be generated beneath 1 m² of surface area can be calculated using the source potential index (SPI = $[S_1+S_2]*h*\rho/1000$, where h is the thickness of the layer and ρ is bulk density; Demaison and Huizinga, 1994).

Assuming that measured depth roughly approximates the true thickness, and assuming a mean value of dry density oil shale of 2.078 t/m^3 (Ignjatovic et al., 2013), the SPI of the upper oil shale layer (26.5-86 m) and the lower oil shale layer (146-176 m) is 14.2 tHC/m^2 and 7.8 t HC/m², respectively.

Oil shale potential

The oil shale potential is often classified based on the oil yield (Fischer assay test; Dyni, 2006). In China low-quality (oil yield 3.5-5 wt.%), medium quality (oil yield 5-10 wt.%), and high quality oil shale (oil yield > 10 wt.%) are distinguished (e.g. Liu et al., 2009; Tao et al., 2010). The oil yield is strongly related to TOC content and organic matter type, expressed by the HI value (e.g. Sun et al., 2013).

Only few oil yield data from Aleksinac oil shales are available. Examinations of oil shale quality regarding oil yield based on Fischer assay tests were performed at the oil refinery in Pancevo (Matic et al., 1959), and laboratories at Faculty of Mathematics and Natural Sciences in Belgrade and Institute of Chemistry, Technology and Metallurgy (IHTM) in Belgrade (Cokorilo et al., 2009). According to the these analysis the homogenous upper oil shale (average kerogen content 18 vol.%) yield on average 8.5 wt.% oil, whereas the organic matter-rich layers in the lower oil shale (average kerogen content 24 vol.%) yield on average 11 wt.% oil. However, the Fischer method is cost-intensive and time-consuming and often results in environmental hazards.

Sun et al. (2013) established equations, which relate oil yield with TOC content, S_2 and HI for oil shales with different quality. If the organic matter composition is uniform, these equations can be used to estimate the oil yield of samples with known TOC content, S_2 and HI. In this section, equations established for oil shales from the Songliao Basin deposited at intermediate water depth are used because of similar type I kerogen type (HI ~765 mgHC/gTOC): Oil yield = 0.82*TOC-0.75; Oil yield = $0.11*S_2$-0.25. Using the above equations, the average oil yield of the upper oil shale layer based on TOC content and S_2 is 11.8 wt.% and 12.2 wt.%, respectively. Even higher oil yields (16.4 wt.% based on TOC; 14.2 wt.% based on S_2) are estimated for the lower oil shale. These data classify the Aleksinac oil shale as high quality according to the Chinese classification.

6. Conclusion

Bulk geochemical analysis, micropetrographic analysis and biomarker analysis of the Aleksinac series were carried out in order to determine the depositional environment of the Aleksinac coal and oil shale. In addition, the amount and origin of organic matter and its petroleum potential is evaluated. Based on this analysis the following conclusions can be drawn:

- Oil shales in the Aleksinac lacustrine basin underlie and overlie the main coal seam. The lower oil shale is alternating with siliciclastic rocks and some thin coal layers, indicating strong variations in depositional environment.
- The lower part of the coal seam was deposited under oxic conditions and represents a low-lying mire environment. A rising water table caused anoxic conditions during the deposition of the upper part of the coal seam. In contrast to the lower part of the coal seam, its upper part is characterised by hydrogen-rich vitrinite and enhanced bacterial biomass. The coal seam was deposited in a vegetation-rich environment, where the input of higher landplants was predominated by angiosperms over gymnosperms.
- Increased subsidence rates caused drowning of the Aleksinac coal seam and the development of a lacustrine environment with the deposition of the 60 m thick upper oil shale. An increasing water depth allowed the establishment of a stratified water column due to differences in salinity. This resulted in a strictly anoxic environment in a mesosalinar lake and the accumulation of a world-class oil shale deposit. Except for some samples, the organic matter is dominated by aquatic organisms and bacteria. Landplants occur in minor amounts. Based on abundant algae-derived liptinite macerals and very high HI values, the organic matter is classified as kerogen type I.
- Increased fresh water influx and an oligotrophic environment prevailed during deposition of bituminous marlstone layers. The primary production of organic matter was dominated by photosynthetic organisms (algae and lake plants) rather than by bacteria.
- According to bulk parameter analysis and vitrinite reflectance, the organic matter of the Aleksinac series is thermally immature.
- Using the terminology of Peters and Cassa (1994), the lower and upper oil shale layers hold a very good to excellent potential to generate oil. Oil shale within the lower oil shale layer yields about 15 wt.% of oil and shows a source potential index of 8 tHC/m^2. The uniform upper oil shale layer yields about 12 wt.% oil. Due to the very high thickness, the source potential index (14 tHC/m^2) of the upper oil shale layer is higher than that in the lower oil shale layer. According to the industrial grade classification, both layers represent a high quality oil shale.

Bibliography

Allix, P., Burnham, A., Fowler, T., Herron, M.; Kleinberg, R., Symington, B., 2011: Coaxing Oil from Shale, Oilfield Review 22

Bartis, J.T., LaTourrette, T., Dixon, L., Peterson, D.J., Cecchine G., 2005: Oil Shale Development in the United States (Prospects and Policy Issues), RAND Corporation

Bechtel, A., Jia, J., Strobl, S.A.I., Sachsenhofer, R.F., Liu, Z., Gratzer, R., Püttmann, W., 2012: Palaeoenvironmental conditions during deposition of the Upper Cretaceous oil shale sequences in the Songliao Basin (NE China): Implications from geochemical analysis, Organic Geochemistry 46, 76-95

Bechtel, A., Püttmann, W., 1997: Palaeoceanography of the early Zechstein Sea during Kupferschiefer deposition in the Lower Rhine basin (Germany): A reappraisal from stable isotope and organic geochemical investigations, Paleogeography, Paleoclimatology, Paleoecology 136, 331-358

Bechtel, A., Sachsenhofer, R.F., Kolcon, I., Gratzer, R., Otto, A., Püttmann, W., 2002: Organic geochemistry of the Lower Miocene Oberdorf lignite (Styria Basin, Austria): its relation to petrography, palynology and the paleoenvironment, International Journal of Coal Geology 51, 31-57

Berner, R.A., 1984: Sedimentary pyrite formation: an update, Geochim. et Cosmochim. Acta 48, 605-615

Bottari, F., Marsili, A., Morelli, I., Pacchiani, M., 1972: Aliphatic and triterpenoid hydrocarbons from ferns, Phytochemistry 11, 2519–2523

Brassell, S.C., Comet, P.A., Eglinton, G., Isaacson, P.J., McEvoy, J., Maxwell, J.R., Thompson, I.D., Tibbetts, P.J.C., Volkman, J.K., 1980: The origin and fate of lipids in the Japan Trench, In: Douglas, A.G., Maxwell, J.R. (Eds.), Advances in Organic Geochemistry, 1979, Pergamon Press, Oxford, 375–392

Brocks, J.J., Love, G.D., Summons, R.E., Knoll, A.H., Logan, G.A., Bowden S.A., 2005: Biomarker evidence for green and purple sulphur bacteria in a stratified Palaeoproterozoic sea, Nature 437, 866-870

Brocks, J.J., Schaeffer, P., 2008: Okenane, a biomarker for purple sulphur bacteria (Chromatiaceae), and other new carotenoid derivates from the 1640 Ma Barney Creek Formation, Gech. et Cosmochim. Acta 72, 1369-1414

Caroll, A.R., Bohacas, K.M., 1999: Stratigraphic classification of ancient lakes: balancing tectonic and climate controls, Geology 27, 99-102

Cokorilo, V., Lilic, N., Purga, J., Milisavljevic, V., 2009: Oil Shale Potential in Serbia, Oil Shale 26(4), 451-462

Connan, J., Cassou, A.M., 1980: Properties of gases and petroleum lipids derived from terrestrial kerogen at various maturation levels, Geochim. et Cosmochim. Acta 44, 1-23

Coplen, T.B., 2011: Guidelines and recommended terms for expression of stable-isotope-ratio and gas-ratio measurements results, Rapid Communications in Mass Spectrometry 25, 2538-2560

Cranwell, P.A., 1977: Organic geochemistry of CamLoch (Sutherland) sediments, Chem. Geol. 20, 205-221

Demaison, G., Huizinga, B.J., 1994: Genetic classification of petroleum systems using three factors: charge, migration and entrapment, in: Magoon, L.B., Dow, W.G. (Eds.), the petroleum system – from source to trap, AAPG Memoir 60, 3-24

Didyk, B. M., Simoneit, B. R. T., Brassell, S. C., and Eglinton, G., 1978: Organic geochemical indicators of paleoenvironmental conditions of sedimentation, Nature 272, 216-222

Diessel, C.F.K., 1992: Coal-Bearing Depositional Systems, Springer, Berlin, 721 p.

Dyni, J.R., 2006: Geology and resources of some world oil-shale deposits, USGS Scientific Investigations Report, U.S. Geological Survey, Reston, Virgina, 4-5

Eglinton, G., Hamilton, R.J., 1967: Leaf epicuticular waxes, Science 156, 1322-1335

Ercegovac, M., 1990: Geology of oil shale (in Serbian), Gradjevinska knjiga, Beograd, 180 pp.

Ercegovac, M., Vitorović, D., Kostić, A., Životić, D., Jovančićević, B., 2009: Geology and Geochemistry of the "Aleksinac" Oil Shale Deposit (Serbia), Joint 61st ICCP/26th TSOP Meeting, Advances in Organic Petrology and Organic Geochemistry

Espitalie, J., La Porte, J.L., Madec, M., Marquis, F., Leplat, P., Paulet, J., Boutefeu, A., 1977: Methode rapide de characterisation des roches meres de leir potential petrolier et de leur degree dèvolution. Revue de l´insitute Francais du Pétrol, 32, 23-42

Espitalie, J., Marquis, F., Barsony, I., 1984: Geochemical logging, In: Voorhess, K.J. (Ed.), Analytical Pyrolysis, Butterworths, Boston, pp. 53-79

Ficken, K.J., Li, B., Swain, D.L., Eglinton, G., 2000: An n-alkane proxy for the sedimentary input of submerged/floating freshwater aquatic macrophytes, Organic Geochemistry 31, 745-749

Gajica, G., Kasanin-Grubin, Mi., Sajnovic, A., Stojanovic, K., Kostic, A., Jovancicevic, B., 2016: Organic geochemical characterization of Aleksinac oil shale deposit (Serbia), Geophysical Research Abstracts, 18, EGU2016-965-2

Hagemann, H.W., Hollerbach, A., 1979: Relationship between the macropetrographic and organic geochemical composition of lignites, In: Douglas,

A.G., Maxwell, J.R. (Eds.), Advances in Organic Geochemistry, Pergamon Press, Oxford, 631–638

Hauke, V., Graff, R., Wehrung, P., Trendel, J.M., Albrecht, P., 1992: Novel triterpene-derives hydrocarbons of arborane/fernane series in sediments – Part I, Tetrahedron 48, 3915-3924

He, W., Lu, S., 1990: A new maturity parameter based on monoaromatic hopanoids, Organic Geochemistry, 16, 1007–1013

Hertelendi, E., Vetö, I.. 1991: The marine photosynthetic carbon isotopic fractionation remained constant during the Early Oligocene, Paleogeography, Paleoclimatology, Paleoecology 83, 333-339

Huang, W.Y., Meinschein, W.G., 1979: Sterols as ecological indicators, Geochim. et Cosmochim. Acta 43, 739-745

Hunt, J.M., 1979: Petroleum Geochemistry and Geology; (Ed.), Gilluily, J., W.H. Freeman and Company, San Francisco, 259-351

Hunt, J.M., 1996: Petroleum Geochemistry and Geology, Freeman and Company

Hutton, A.C., 1987: Petrographic classification of oil shales, International Journal of Coal Geology 8, 203–231

Hutton, A.C., 1988: Organic petrography of oil shales, U.S. Geological Survey short course, January 25–29, Denver, Colo., 306 p., 16 p

Hutton, A.C., 1991: Classification, organic petrography and geochemistry of oil shale, in Proceedings 1990 Eastern Oil Shale Symposium, Lexington, University of Kentucky Institute for Mining and Minerals Research, 163–172

Ignjatovic, M., Rajkovic, R., Ignjatovic, S., Ignjatovic, L. D., Kricak, L., Pantovic, R., 2013: Determination of optimal countours of open pit mine during oil shale exploration, by Minex 5.5.3. program, Journal of process management – new technologies 1(2)

Jelenkovic, R., Kostic, A., Zivotic, D., Ercegovac, M., 2008: Mineral resources of Serbia, Geologica Carpathica 59, 345-361

Jiang, Z. and Fowler, M. G. 1986: Carotenoid-derived alkanes in oils from northwestern China, Organic Geochemistry 10, 831–839

Karrer, W., Cherbuliez, E., Eugster, C.H., 1977: Konstitution und Vorkommen der organischen Pflanzenstoffe, Ergänzungsband I., Birkhäuser, Basel, Stuttgart, 1038 pp.

Kasanin-Grubin, M., 1996: Sedimentologija serje uljnih skrilajaca Aleksinackog jezerskog basena, Maistrarska etza, Rudarsko-geoloski fakultet, Univerzitet u Beogradu, 155 str.

Kasanin-Grubin, M., Glumicic, T., Jovancicevic, B., Obradovic, J., 1997: Investigation of origin and sedimentation conditions of the Aleksinac oil shales on

the basis of inorganic and organic matter composition (in Serbian), Annales Géologiques de la Péninsule Balkanique 61, 325-348

Knaus, E., Killen, J., Biglarbigi, K., Crawford, P., 2010: An Overview of Oil Shale Resources, in: Ogunsola, O.I., Hartstein A.M., Ogunsola O. (eds): Oil Shale: A Solution to the Liquid Fuel Dilemma, Washington DC: American Chemical Society, ACS Symposium Series, 1032, 3-20

Kodner, R.B., Pearson, A., Summons, R.E., Knoll, A.H., 2008: Sterols in red and green algae: quantification, phylogeny, and relevance for the interpretation of geologic steranes, Geobiology 6(4), 411-420

Krstic, N., 1996: Neogene of central Serbia, International Geological Correlation Programme, Special publication of Geoinsitute, No 19

Lambiase, J.J., 1990: A model for tectonic control of lacustrine stratigraphic sequences in continental rift basins, in: Katz, B.J. (Ed.), Lacustrine basin exploration: case studies and modern analogs, AAPG Memoir 50, 265-276

Lichtfouse, E., Derenne, S., Mariotti A., Largean, C., 1994: Organic Geochemistry 22(6), 1023-1027

Liu, Z.J., Yang, H.L., Dong, Q.S., Zhu, J.W., Guo, W., Ye, S.Q., Liu, R., Meng, Q.T., Zhang, H.L., Gan, S.C., 2009: Oil Shale in China, Petroleum Industry Press, Beijing, 343 pp. in Chinese with English abstract

Logan, G.A., Eglinton, G., 1994: Biogeochemistry of the Miocene lacustrine deposit at Clarkia, northern Idaho, U.S.A., Organic Geochemistry 21, 857–870

Marovic, M., Krstic, N., Stanic, N., Cvetkovic, V., Petrovic, M., 1999: The evolution of Neogene sedimentation provinces of central Balkan peninsula, Radovi Geoinstituta (Bulletin of Geointitute), Beograd 36, 25-94

Mastalerz, M., Wilks, R., Bustin, R.M., 1993: Variation in vitrinite chemistry as a function of associated liptinite content; a microprobe and FT-IR investigation, Organic Geochemistry 20, 555– 562

Matić, D., Lazarević, J., Mijatović. I., 1959: Testing of Aleksinac oil shale in semiindustrial facility in Pancevo town, Chemical Industry, 13(10), 1617–1625

McKirdy, D.M., Cox, R.E., Volkman, J.K., Howell, V.J., 1986: Botryococcane in a new class of Australian nonmarine crude oils, Nature 320, 57

Moldowan, J. M., Dahl, J., Huizinga, B. J., Fago, F. J., Hickey, L. J., Peakman, T. M., and Taylor, D. W., 1994: The molecular fossil record of oleanane and its relation to angiosperms, Science 265, 768-771

Moravic, M., Djokovic I., Pesic, L., Radovanovic, L., Tojic, M., Gerzina, N., 2002: Neotectonics and seismicity of the southern margin of the Pannonian basin in Serbia, EGU Stephan Mueller Special Publication Series, 3, 277-295

Mukhopadhyay, P. K., Dow, W. G., 1994: Vitrinite Reflectance as a Maturity Parameter: Applications and Limitations, volume 570 of ACS symposium series, American Chemical Society

Naafs, B.D.A., 2016: Introduction in stable carbon isotopes, www.organicgeochemistry.me/biomarker-proxies-explained/464-2

Noble, R.A., Alexander, R., Kagi, R.I., Knox, J., 1985: Tetracyclic diterpenoid hydrocarbons in some Australian coals, sediments and crude oils, Geochim. Cosmochim. Acta 49, 2141–2147

Novković, M., Grgurović, D., 1992: A study of actual geological-economic valorisation of some oil shale deposits and findings in Serbia, Documentation of Geozavod, Belgrade

Obradović, J., Djurdjević - Colson, J., Vasić, N., 1997 Phytogenic lacustrine sedimentation - oil shales in Neogene from Serbia, Yugoslavia, Journal of Paleolimnology 18, 351-364

Obradović, J., Vasić, N., Kasanin-Grubin, M., Grubin, N., 2000: Neogene lacustrine sediments and authigenic minerals geochemical characteristics, Ann. Geol. Penins. Balk. 63, 135-154

Ourrison, G., Albrecht, P., Rohmer, M., 1979: The hopanoids: palaeo-chemistry and biochemistry of a group of natural products, Pure Appl. Chem. 51, 709–729

Paull, R., Michaelsen, B. H. and McKirdy, D. M., 1998 Fernenes and other triterpenoid hydrocarbons in Dicroidium-bearing Triassic mudstones and coals from South Australia, Organic Geochemistry 29, 1331–1343

Peters, K. E., Cassa, M. R. 1994: Applied source rock geochemistry, In: The Petroleum System – From Source to Trap (L. B. Magoon and W. G. Dow, eds.), American Association of Petroleum Geologists, Tulsa, OK, 93–117

Peters, K. E., Clutson, M. J., and Robertson, G., 1999: Mixed marine and lacustrine input to an oil-cemented sandstone breccia from Brora, Scotland, Organic Geochemistry 30, 237-248

Peters, K. E., Walters, C. C., and Moldowan, J. M., 2005b: The Biomarker Guide: Biomarkers and Isotopes in the Environment and Human History, volume 1 of The Biomarker Guide, Cambridge University Press

Peters, K.E., 1986: Guidlines for evaluating petroleum source rocks using programmed pyrolysis, AAPG Bulletin 70, 318-329

Peters, K.E., 2000: Petroleum tricyclic terpanes: predicted physicochemical behavior from molecular mechanics calculations, Organic Geochemistry 31(6), 497-507

Peters, K.E., Walters, C.C., Moldowan, J.M., 2005: The Biomarker Guide - Biomarkers and Isotopes in Petroleum Exploration and Earth History, Cambridge University Press, New York

Petković, K. & Novković, M., 1975: Bituminous (oil) shales of Serbia (in Serbian), Geology of Serbia, Caustobioliths, VII, 197-210

Philp, R.P., 1985: Fossil fuel biomarkers, Applications and spectra, Meth. Geochem. Geophys. 23, 1–294

Radke, M., Willsch, H., Welte, D.H., 1980: Preparative hydrocarbon group type determination by automated medium pressure liquid chromatography; Anal. Chem. 52 (1980), 406–411

Repeta, D. J. 1989: Carotenoid diagenesis in recent marine sediments – II. Degradation of fucoxanthin to loliolide, Geochim. et Cosmochim. Acta 53, 699–707

Repeta, D. J. and Gagosian, R. B., 1987: Carotenoid diagenesis in recent marine sediments – I. The Peru contenental shelf (15°S, 75°W), Geochim. et Cosmochim. Acta 51, 1001–1009

Rohmer, M., Bisseret, P., 1994: Hopanoid and other polyterpenoid biosynthesis in eubacteria, ACS Symp. Ser. 562, 31–43

Rohmer, M., Bouvier-Nave, P., Ourisson, G., 1984: Distribution of hopanoid triterpenes in prokaryotes, Journal of General Microbiology 130, 1137-1150

Rullkötter, J., Peakman, T.M., ten Haven, H.L., 1994: Early diagenesis of terrigenous triterpenoids and its implications for petroleum geochemistry, Organic Geochemistry 21, 215–233

Sachsenhofer, R.F., 2000: Geodynamic controls on deposition and maturation of coal in the Eastern Alps, in: Neubauer, F., Höck, V. (Eds.), Aspects of Geology in Austria, Mitteilungen der Österreichischen Geologischen Gesellschaft 92, 185-194

Sachsenhofer, R.F., Bechtel, A., Reischenbacher, D., Weiss, A., 2003: Evolution of lacustrine systems along the Miocene Mur-Mürz fault system (Eastern Alps, Austria) and implications on source rocks in pull apart basins, Marine and Petroleum Geology 20, 83-110

Savage, H. K., 1967: The Rock That Burns: (Privately published), Printed by Pruett Press, Boulder, Colorado

Schnitzler, M., Neyroud, J.A., 1975: Alkanes and fatty acids in humic substances, Fuel 54, 17–19

Sinninghe Damste, J. S., Kenig, F., Koopmans, M. P., et al., 1995: Evidence for gammacerane as an indicator of water-column stratification, Geochim. et Cosmochim. Acta 59, 1895-1900

Sun, P., Liu, Z., Gratzer, R., Xu, Y., Liu, R., Li, B., Meng, Q., Xu, J., 2013: Oil yield and bulk geochmical parameters of oil shales from the Songliao and Huadian basins, China: A grade classification approach, Oil shale 30(3), 402-418

Symington, W.A., Kaminsky, R.D., Meurer, W.P., Otten, G.A., Thomas, M.M., Yeakel, J.D., 2010: "ExxonMobile's Electrofac™ Process for In Situ Oil Shale Conversion," in Ogunsola, O.I., Hatstein, A.M. and Ogunsola, O. (eds): Oil Shale: A

Solution to the Liquid Fuel Dilemma, Washington DC: American Chemical Society, ACS Symposium Series 1032, 185-221

Tao, S., Tang, D. Z., Li, J. J., Xu, H., Li, S., Chen, X. Z, 2010: Indexes in evaluating the grade of Bogda Mountain oil shale in China, Oil Shale 27(2), 179-189

Taylor, G.H., Teichmüller, M., Davis, A., Diessel, C.F.K., Littke, R., Robert, P., 1998: Organic Petrology, Gebrüder Borntraeger, Berlin, 704

ten Haven, H.L., Peakman, T.M., Rullkötter, J., 1992: Early diagenetic transformation of higher-plant triterpenoids in deep-sea sediments from Baffin Bay, Geochim. et Cosmochim. Acta 56, 2001–2024

Tissot, B. P., Welte, D. H., 1984: Petroleum Formation and Occurrence, Springer-Verlag, Berlin

Tissot, B.P., Welte, D.H., 1984: Petroleum Formation and Occurrence, 2nd edition, Springer-Verlag, Berlin

Tsuda, Y., Tabata, Y. and Ichinohe, Y. 1980: Lycopodium triterpenoids (10), Triterpenoid constituents of Lycopodium wightianum collected in Borneo, Chemical and Pharmaceutical Bulletin, 28, 3275–3282

Vass, D., Krstić, N., Milićka, J., Kovacova-Slamkova, M., Obradović, J. & Grgurević, D., 2006: Organic matter and fossil content in Serbian oil shales: Comparison with oil shales of Central Europe, Slovac Geologic Magazine 12 (2), 147–158

Volkman, J. K. and Maxwell, J. R. 1986: Acyclic isoprenoids as biological markers, In: Johns, R.B. (Ed.) Biological Markers in the Sedimentary Record, Elsevier, New York, 1–42

Volkman, J.K., 1986: A review of sterol markers for marine and terrigenous organic matter, Org. Geochem, 9, 83–99

Volkman, J.K., Allen, D.I., Stevenson P.L., Burton, H.R., 1986: Bacterial and algal hydrocarbons from a saline Antarctic lake, Ace Lake, Org. Geochem, 10, 671–681

Wakeham, S.G., 1990: Algal and bacterial hydrocarbons in particulate material and interfacial sediment of the Cariaco Trench, Geochim. et Cosmochim. Acta 54, 1325–1336

Wolff, G.A., Ruskin, N., Marshall, J.D., 1992: Biogeochemistry of an early diagenetic concretion from the Birchi Bed (L. Lias, W. Dorset, U.K.), Organic Geochemistry 19, 431–444

Youngquist, W., 1998: Shale Oil – The Elusive Energy, M. King Hubbert Center, Petroleum Engineering Department, Colorado School of Mines, 1

List of Figures

List of Tables

Appendix

Organic Petrology – Microphotographs – upper oil shale

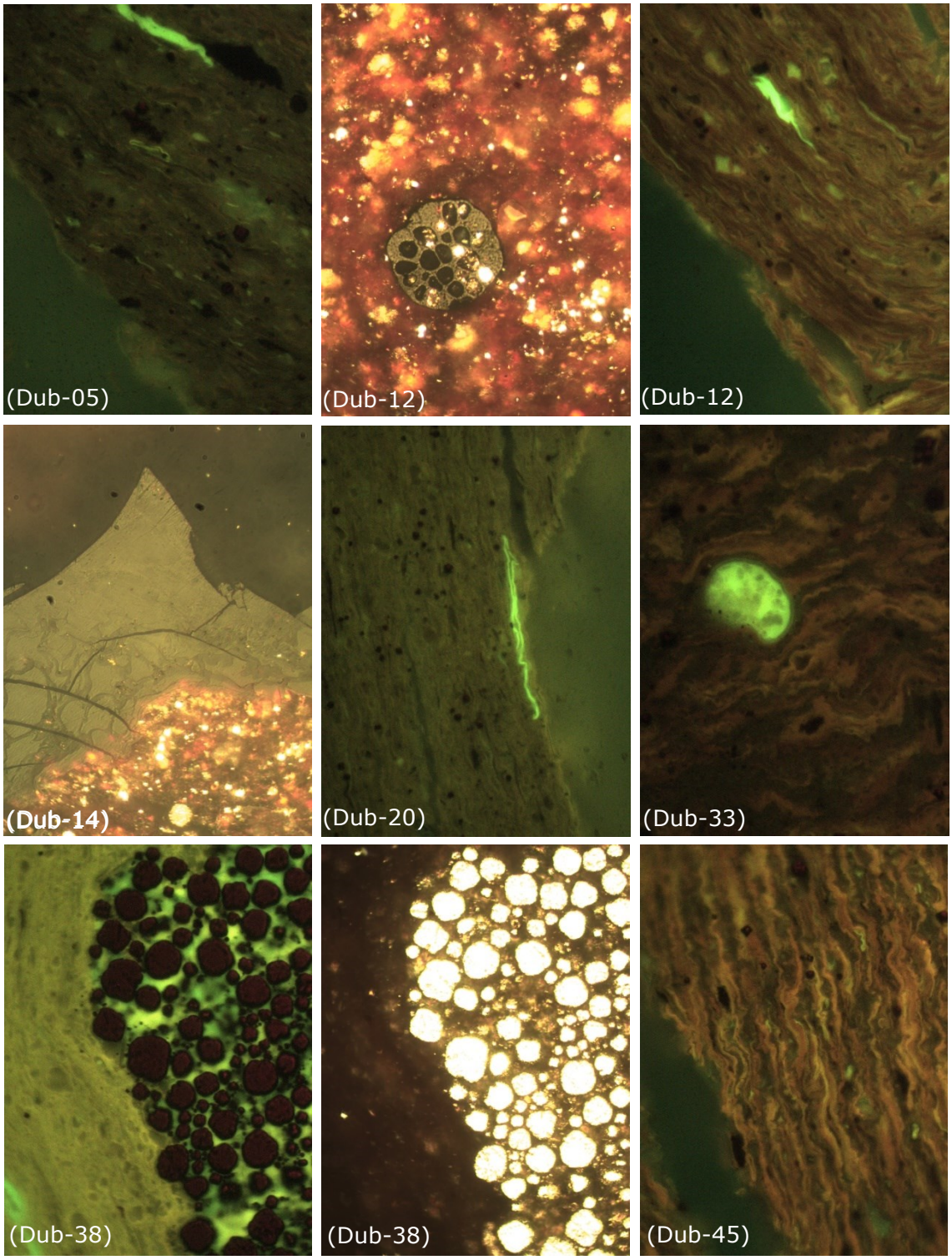

Organic Petrology – Microphotographs – coal seam